Calculations of Hartree-Fock Polarizabilities for Some Simple Atoms and Molecules, and Their Practicality*

VINCENT P. GUTSCHICK** AND VINCENT McKOY†

Arthur Amos Noyes Laboratory of Chemical Physics

California Institute of Technology

Pasadena, California 91109

Hartree-Fock electric polarizabilities have been calculated for H_2, He, Li, Be, LiH, and N_2. Perturbation theory with all the coupling terms was employed variationally for the first five, using a variety of basis sets for each. Each basis for the perturbation calculations was composed of a zero-order set, plus a first-order set (appropriate to the direction of polarization, for the molecules). The two sets are disjoint to ensure identical zero-order functions for the two molecular polarizability components and, hence, reliable anisotropy values. Nonorthogonal theory as formulated by T. P. Das and K. J. Duff [Phys. Rev. 168, 43 (1968)], assuming exact zero-order orbitals, was used for LiH. For practical reasons, the nitrogen molecule was treated by the fully self-consistent approach

---

* Contribution No.

** National Science Foundation Predoctoral Fellow, 1966-1970.

† Alfred P. Sloan Foundation Fellow.

which does not distinguish orders of perturbation. The results for all six species are in very good agreement with experiment, reflecting both a reliable choice of polarization functions and, more significantly, the basic accuracy of the Hartree-Fock method for the static charge distributions, both unperturbed and perturbed by an electric field.

I. INTRODUCTION AND THEORY

Among variational theories of molecular electronic structure, the Hartree-Fock theory has proved particularly valuable for a practical understanding of such properties as chemical binding, electric multipole moments, and x-ray scattering. It provides the most tractable method of calculating first-order properties under external or internal one-electron perturbations, either developed explicitly in orders of perturbation theory or in the fully self-consistent method. Electric polarizabilities,[1-4] and magnetic properties[5] such as spin coupling, chemical shift, and susceptibility have been treated with the theory. The accuracy and consistency of first-order properties are poorer than those of zero-order properties. Most often this is due to use of explicit approximations in solving the first-order perturbation equations, or to the inaccuracies of the zero-order molecular orbitals (MO's) which may undermine the variational principle for the second-order energy. Theoretical studies using many-body theory[6, 7] indicate that the Hartree-Fock theory itself is basically sound for static or zero-frequency properties, and we do not intend to draw further conclusions along this line. Rather, we have performed representative calculations of static electric polarizabilities for small atoms and molecules to underscore the basic soundness of perturbed Hartree-Fock theory, giving important and practical guidelines for selecting the variational basis sets for the first-order wavefunction.

Our first studies were on H_2 and the atoms He, Li, Be using a variety of simple wavefunctions constructed from Slater type orbitals (STO's). For such few-electron species, the problem is best solved by constructing explicit first-order perturbation equations for the perturbation ϕ_i^1 to the unperturbed molecular orbitals ϕ_i^0. The unperturbed electronic Hamiltonian contains one-electron terms $\underline{h_i^0}$ and two-electron terms $\underline{g_{ij}} = 1/\underline{r_{ij}}$ (in atomic units),

$$H^0 = \sum_i h_i^0 + \sum_{i<j} \sum g_{ij} \quad . \tag{1}$$

The perturbation due to an electric field $\mathcal{E}$ along the axis $\underline{k}$ is

$$H^1 = \mathcal{E} \sum h_i^1 = \mathcal{E} \sum r_{ik},$$

and the zero-order and first-order Hartree-Fock equations are respectively

$$(h^0 + \sum_j \langle \phi_j^0 | \cdot | \phi_j^0 \rangle - \epsilon_i^0) \phi_i^0 = 0 \tag{2a}$$

$$(h^0 + \sum_j \langle \phi_j^0 | \cdot | \phi_j^0 \rangle - \epsilon_i^0) \phi_i^1$$

$$+ (h^1 + \sum_j [\langle \phi_j^1 | \cdot | \phi_j^0 \rangle + \langle \phi_j^0 | \cdot | \phi_j^1 \rangle] - \epsilon_i^1) \phi_i^0 = 0, \tag{2b}$$

with the usual convention of order-by-order orthogonality,

$$\langle \phi_i^0 | \phi_j^0 \rangle = \delta_{ij} \tag{3a}$$

$$\langle \phi_i^0 | \phi_j^1 \rangle = 0. \tag{3b}$$

Here we use the shorthand notation

$$\langle a | \cdot | b \rangle c = \langle a(j) | g_{ij} | b(j) \rangle c(i) - \langle a(j) | g_{ij} | c(j) \rangle b(i). \tag{4}$$

The zero-order equation is commonly solved variationally using STO's (χ_p^0) centered on the nuclei,

$$\phi_i^0 = \sum_p c_{ip}^0 \chi_p^0. \tag{5}$$

The first-order equation may be solved variationally in a similar way. Operationally, this means making Eq. (2b) hold for all projections with the first-order basis set $\{\chi^1\}$,

$$\langle \chi_p^1 | h^0 + \sum_j \langle \phi_j^0 | \cdot | \phi_j^0 \rangle - \epsilon_i^0 | \phi_i^1 \rangle + \langle \chi_p^1 | h^1 + \sum_j [\langle \phi_j^0 | \cdot | \phi_j^1 \rangle + \langle \phi_j^1 | \cdot | \phi_j^0 \rangle - \epsilon_i^1 | \phi_i^0 \rangle = 0, \tag{6}$$

for all p and i.

Substitution of the appropriate basis expansions for the ϕ_i^1, including the explicit forms for the matrix elements ϵ_i^1, yields linear equations for the first-order coefficients c_{ip}^1. This is equivalent to minimizing the second-order energy, assuming the exactness of the zero-order solution in the total basis $\{\chi\} = \{\chi^0\} + \{\chi^1\}$,

$$\langle \chi_r | h^0 + \sum_j \langle \phi_j^0 | \cdot | \phi_j^0 \rangle - \epsilon_i^0 | \phi_i^0 \rangle = 0 \qquad (7)$$

for all r.

Given a zero-order basis $\{\chi^0\}$ and the direction or axis of polarization k, the polarization functions $\{\chi^1\}_k$ can be picked judiciously to include all important shifts in orbital amplitudes while remaining few in number. A major part of the work reported herein concerns just such choice of the basis. We have shown that the distortion of ϕ_i^0 can be adequately described by allowing each atomic orbital in the MO to distort in the electric field as a pure hydrogenic orbital would distort. For the H_2 molecule and the three atoms He, Li, Be, our work is further simplified since the polarization functions are automatically of a different symmetry from the occupied orbitals: σ_u vs. σ_g for H_2, and p vs. s for the atoms. The calculations proceed very straightforwardly to the second-order energy in the electric field ,

$$\mathcal{E}^2 E^{(2)} = \mathcal{E}^2 \sum_i \langle \phi_i^1 | h^1 | \phi_i^0 \rangle, \qquad (8a)$$

which directly measures the polarizability as

$$E^{(2)} = -\tfrac{1}{2}\alpha. \tag{8b}$$

We obtained excellent agreement with most reliable values, either experimental or theoretical. The results were markedly insensitive to the choice of zero- and first-order bases.

We were encouraged to try molecules of lower symmetry and more electrons. The first case was LiH, previously treated by Lipscomb and Stevens[1] in similar fashion. Now our simple expedient of distorting the atomic orbital basis functions as if they described hydrogenic atoms yields a first-order basis composed of functions not automatically orthogonal to the occupied orbitals by symmetry. We can Schmidt orthogonalize the χ_p^1 to the χ_q^0 before doing any perturbation calculations, but this involves much manipulation of the raw one- and two-electron integrals over basis functions. The nonorthogonal perturbation formalism of Das and Duff[8] performs instead a symmetric deorthogonalization in the matrix equations (6). They perform the deorthogonalization before separating orders of perturbation in the Hartree-Fock equations and minimizing the second-order energy with respect to the ϕ_i^1. Thus, they obtain extra terms in the first-order equation due to inexactness of the ϕ_i^0 in the augmented basis $\{\chi^0\} + \{\chi^1\}_k$: Eq. (7) is not satisfied. Most often these terms are small and can be dropped much as Das and Duff do in their final presentation. We then have at hand a formalism for computing separately the two polarizability

components $\alpha_{\underline{k}}$ ($\alpha_{\underline{zz}}$ and $\alpha_{\underline{xx}}$) in small total bases while retaining reliability of the anisotropy $\alpha_{\underline{k}} - \alpha_{\underline{\ell}}$.

Finally we tried the N_2 molecule, with its many electrons and many occupied symmetry types of orbitals. Practical zero-order bases of Gaussian type orbitals (GTO's) do not keep the ϕ_i^0-inexactness terms in the perturbation equations sufficiently small any more. Even in LiH, GTO's cause this problem. The inexactness terms are too prolific to include. The problem is avoided by shifting both zero- and first-order calculations to the common, enlarged basis $\{\chi^0\} + \{\chi^1\}_k$. The unoccupied virtual orbitals from zero-order can then act as the new χ_p^1. To once more avoid much manipulating of two-electron integrals, we abandoned the perturbation formalism in favor of the fully self-consistent approach, equivalent at low fields $\mathcal{E}$. The basic Hartree-Fock equations unseparated into orders are solved, given a finite electric field. The field is small enough such that $\phi_i \approx \phi_i^0 + \mathcal{E}\phi_i^1$ and $\underline{E} \simeq \underline{E^0} + \mathcal{E}\underline{E^{(1)}} + \mathcal{E}^2\underline{E^{(2)}}$ and higher orders are negligible (for N_2, $\underline{E^{(1)}} = 0$, too). Now, if one computed the two polarizability components separately, the anisotropy $\alpha_k - \alpha_\ell$ would be less reliable because the unperturbed energy is doubtlessly shifted differently in the two different total bases $\{\chi^0\} + \{\chi^1\}_k$, $\{\chi^0\} + \{\chi^1\}_\ell$. We thus prefer one large basis $\{\chi^0\} + \{\chi^1\}_k + \{\chi^1\}_\ell$ for all calculations. Fortunately, for N_2 a good zero-order basis $\{\chi^0\}$ already contains many functions which may also act as polarization functions and $\{\chi^0\}$ is not greatly enlarged by adding the nonredundant parts of $\{\chi^1\}_k$ and $\{\chi^1\}_\ell$.

Beyond the approximation of finite basis expansion for the molecular orbitals ϕ_i (in all orders), several approximations to Hartree-Fock theory have been proposed. The explicit perturbation equations (2b) are altered in these approximations to eliminate the need for all or most of the two-electron integrals over basis functions. Dalgarno[9] has discussed these methods, and the approximations have been evaluated relative to the "full theory" by Langhoff, Karplus, and Hurst.[10] While these theories save most of the effort in evaluating a first-order property, they consistently undervalue the polarizability to an unpredictable extent. We wish to test the accuracy of full Hartree-Fock theory which neglects only instantaneous correlation. We do not consider further the approximations to its perturbation formalism.

II. APPLICATIONS AND RESULTS

Many polarizability, magnetic susceptibility, and magnetic shielding calculations have been done for H_2, by all manners of perturbation theory and with all types of unperturbed wavefunctions. We focused on the simpler zero-order wavefunctions, the Coulson[11] and Ransil[12] Hartree-Fock (HF) functions and the Wang[13] valence-bond (VB) function. The Coulson and Wang wavefunctions use only one 1s atomic orbital on each center, while the Ransil function includes one 2s and one $2p_z$ in addition. In each case the wavefunction was perturbed by letting each basis function χ_p^0 assume the variational form (there is only one MO).

$$\chi_p \rightarrow \chi_p^0 + c\mathcal{E}\chi_p^1, \tag{9}$$

with c a variational constant. For the two HF wavefunctions this is equivalent to the perturbed HF formalism outlined previously,

$$\phi_i \rightarrow \phi_i^0 + \mathcal{E}\phi_i^1.$$

The analogous VB treatment involves straightforward minimization of the second-order energy.

The χ_p^1 were selected initially as solutions of the hydrogen-like atom in an electric field with χ_p^0 as the unperturbed wavefunction,

$$(-\tfrac{1}{2}\nabla^2 + \frac{Z}{r} + \frac{Z^2}{2n_p^2})\chi_p^1 + (-\zeta_p r_k - \epsilon_{pk}^1)\chi_p^0 = 0. \tag{10}$$

Here n_p is the principal quantum number of χ^0_p, ζ_p is the orbital exponent, Z is the effective nuclear charge $n_p\zeta_p$, and ϵ^1_{pk} is the first-order energy associated with the perturbation $-\mathcal{E}r_k$ along the Cartesian axis k. Thus a 1s STO in a z-directed field yields as χ^1_p a linear combination of $2p_z$ and $3p_z$ of the same ζ_p; a 2s Slater--a $2p_z$, $3p_z$, and $4p_z$ combination; a $2p_x$--a $3d_{xz}$ and $4d_{xz}$; a $2p_z$--a 1s, 2s, 3s, 4s, $3d_{3z^2-r^2}$, and $4d_{3z^2-r^2}$. All of the hydrogen molecule trials used the STO's in the χ^1_p frozen in their original linear combinations, even if, for example, only $2p_z$ and $4p_z$ were used for the 2s polarization. The molecular calculations on LiH and N_2 in contrast used Eq. (10) simply as an indication of important primitive basis functions, STO or GTO, to include in bases unconstrained by any linear combinations.

The results are in Table I. Trials A, B, and E are most relevant, as they compare three different simple wavefunctions under essentially complete polarization according to Eq. (11). They are compared to the extremely accurate polarizabilities of Kolos and Wolniewicz[14] who used a 54-term zero-order wavefunction and 34 terms in first order. Quadratic interpolation was done to the internuclear distances R used in our calculations. Sufficiently accurate experimental polarizabilities are only available at optical frequencies. The insensitivity of our results to the choice of the zero-order functions along with the first order wavefunction chosen according to Eq. (11), and their agreement with experiment, is very encouraging. Result C shows that optimization of the exponents for

polarization functions is unnecessary, and case D indicates a need for polarizing the majority of the zero-order basis.

The He, Li, and Be atoms were treated next, using Clementi's[15] unperturbed wavefunctions computed in double-zeta basis sets. An accurate He polarizability, α = 1.397 a.u., has been obtained by Johnston, et al.[16] by extrapolation of the experimental dielectric constant to zero pressure. Dutta, et al.,[17] have used many-body theory on He and found α = 1.407 a.u. Our result of 1.319 a.u. is 6.0% low relative to the experiments, the first in a trend to undervaluing the correct polarizability for atoms. The best Li polarizability was determined by Fues[18] using the Stark splitting in lithium metal; molecular beam measurements use single atoms rather than bulk metal but have been far less precise. Our Li wavefunction, which is of unrestricted Hartree-Fock form, gave a result of 167.6 a.u., 7.9% below the experimental value of 182 a.u. Beryllium atom provided our greatest success, as it has for several other calculations using Hartree-Fock theory; the computed value of 45.28 a.u. lies only 3.2% lower than the accurate many-body result of 46.77 a.u. due to Kelly.[7] No experimental results are reliable. All three atomic calculations showed negligible, usually negative contributions to α by the core orbitals, as might be expected.

The LiH molecule, as a heteronuclear species with two electronic shells, provides a somewhat better test of Hartree-Fock theory, particularly its nonorthogonal formulation discussed in the previous section. Ransil's[19] wavefunction was chosen for zero order

at the experimental internuclear distance $\underline{R} = \underline{R_e} = 3.015$ a.u. The perpendicular polarization was represented by the full set of four hydrogenic-model polarization functions χ_p^1--see Eq. (11). Standard orthogonal perturbation theory[20] could be used for $\alpha_\perp$, yielding the value 26.22 a.u. This agrees well with the most reliable theoretical estimate of 27.00 a.u. by Stevens and Lipscomb.[1] The parallel component is more difficult, requiring nonorthogonal theory. We chose to test here many of our ideas on the adequacy of polarization functions, and so we pooled all 13 primitive χ_p^1 as unconstrained individual STO's, plus the two virtuals from zero-order. The complete basis yielded $\alpha_\parallel = 25.29$. Stevens and Lipscomb[1] did not compute $\alpha_\parallel$ because of the change of zero-order basis necessary to retain the orthogonal perturbation theory. Kolker and Karplus[2] have made cruder calculations, $\alpha_\parallel = 25.38$ a.u. and $\alpha_\perp = 34.42$ a.u., which are in poor agreement with ours, but at least show a negative anisotropy $\alpha_\parallel - \alpha_\perp = -9.04$ a.u.; our value is -0.93 a.u. We could conclude that the $\underline{2p}, \underline{3p}$-like orbitals from polarization of the tight $\underline{1s_{Li}}$, the $\underline{2p}$ from the $2s_{Li}$ (nearly redundant with the zero-order $\underline{2p}$), and the $\underline{2s}$ from the $\underline{2p_{Li}}$ polarization were all unimportant. This new basis $\{\chi^1\}$ yielded $\alpha_\perp = 25.04$ to confirm our judgment. Many other deletions were tried, with a nine-function set being the smallest to give a good result: the two virtuals plus the $\underline{3p}, \underline{4p}$ STO's from the $\underline{2s_{Li}}$, the $\underline{1s}, \underline{3s}, \underline{3d}$ from the $\underline{2p_{Li}}$, and the $\underline{2p}, \underline{3p}$ from the $\underline{2s_H}$ gave $\alpha_\parallel = 24.63$ a.u. In all these calculations the inner core orbital was seen to back-polarize slightly, following the trend of the atoms.

The N_2 molecule is tractable only in a Guassian basis set due to the large number of two-center, two-electron integrals required. For experience in selecting the $\{\chi_p^1\}$, we returned to the LiH molecule in a GTO basis. We attempted to reproduce the non-orthogonal perturbation theory results for STO's, choosing Gaussians contracted by Huzinaga's[21] prescription to mimic the STO's for atoms. While the zero-order energy was close, the dipole moment was poorer and the polarizability using just the two virtual orbitals was two-thirds that obtained using the STO's. This indicates poor tails for the Gaussian wavefunctions. We tried to add to the non-orthogonal perturbation theory the extra terms due to inexactness of the ϕ_i^0, but these proliferated wildly. Instead we settled for an equivalent fully-self-consistent approach discussed earlier. The polarizability is taken from the ratio of the induced dipole moment to the electric field, possibly extrapolated to zero field for greater accuracy. We did not do such extrapolations, since the larger inherent error of Hartree-Fock theory does not warrant it.

We began our LiH calculations with a very large basis of zz functions covering a full range of exponents in 1s, 2p, and 3d GTO's for Li and 1s, 2p for H. By trial and error we pared the basis to 15 functions, which yielded $\alpha_{\|} = 21.06$, $\alpha_{\perp} = 22.56$. The anisotropy is negative as for STO's, but absolute magnitudes are down about 15%, somewhat disturbingly. Perhaps lack of closely-spaced exponents for the Gaussians is responsible, as this disallows construction of more diffuse functions with radial nodes.

Proceeding to N_2, we built from the zero-order basis of Dunning[22] consisting of 13 contracted GTO's (22 primitives) on each nitrogen, four of the s-type, three of each p-component. The calculations were done at the experimental internuclear distance, 2.068 a.u. We added on each center a diffuse 1s (ζ = 0.0800) for z-polarization of the $2p_z$ or x-polarization of the $2p_x$; a similarly diffuse 2p (0.0800) of all three directions for x and z-polarizations of the σ orbitals; and a host of d-functions all of moderately diffuse exponent 0.200. Among the d-functions the two-center linear combination $XX_A + XX_B$ covers the x-field on π_u^x orbital; $YY_A + YY_B$ is simply the complement to the above for the σ-orbital balance; $XY_A + XY_B$ covers the x-field on π_u^y, while $YZ_A + YZ_B$ is for the z-field; XZ_A and XZ_B are used independently to represent the x-polarization of σ_g, σ_u and the z-polarization of the π_u^x orbital.

The computed $\alpha_{\parallel}$ and $\alpha_{\perp}$ are 14.97 and 9.46 a.u., respectively. It is of practical interest that it was extremely difficult to obtain convergence of the SCF procedure for the z-polarized case. Three-point extrapolation[23] by the e_k procedure for oscillating and diverging series was used, as outlined by Petersson and McKoy.[23] The comparable experimental values are $\alpha_{\parallel}$ = 16.06 and $\alpha_{\perp}$ = 9.78 a.u. obtained dynamically with Na D light.[24] Dispersion corrections may be estimated to give static polarizabilities of 15.9 and 9.7 a.u. The agreement of theory and experiment is quite remarkable. It may be partly fortuitous, due to a 5-15% underestimation of α when using a GTO basis, or to increased inaccuracy of the highly polarizable valence orbitals in systems of many electrons. One more

interesting feature of the N_2 polarization is the coupling of orbitals in pairs under the field influence. The $1\sigma_g$, $1\sigma_u$ orbitals are essentially unpolarized for both field directions. For an $\underline{x}$-field, the $2\sigma_g$ gives 11.4% of the polarizability and the $2\sigma_u$ 31.0%; the $3\sigma_g$ and $1\pi_u^x$ couple, with to latter anti-polarizing, to give another 42.4%; and the $1\pi_u^y$ yields the last 15.2%. In a $\underline{z}$-field the $2\sigma_g$ contributes 4.1%; the $2\sigma_u$-$3\sigma_g$ coupled give 26.0%; the $1\pi_u^x$ 31.1%; and the $1\pi_u^y$ 38.8%. The disparity of the last two contributions is due to a slight inequivalence in the zero-order descriptions of the two orbitals: the $\underline{xz_A}$, $\underline{xz_B}$ polarization functions also enter into the unperturbed $1\pi_u^x$.

REFERENCES

[1]R. M. Stevens and W. N. Lipscomb, J. Chem. Phys. 40, 2238 (1964).

[2]H. J. Kolker and M. Karplus, ibid. 39, 2011 (1963).

[3]V. G. Kaveeshar, K. T. Chung, and R. P. Hurst, Phys. Rev. 172, 35 (1968).

[4]G. P. Arrighini, M. Maestro, and R. Moccia, Chem. Phys. Letters 1, 242 (1967).

[5]H. F. Hameka, Advanced Quantum Mechanics (Addison-Wesley, Reading, Mass., 1965).

[6]T. C. Caves and M. Karplus, J. Chem. Phys. 50, 3649 (1969).

[7]H. P. Kelly, Phys. Rev. 136, B896 (1964).

[8]T. P. Das and K. J. Duff, Phys. Rev. 168, 43 (1968).

[9]A. Dalgarno, Adv. Phys. 11, 281 (1962); with J. M. McNamee, J. Chem. Phys. 35, 1517 (1961).

[10]P. W. Langhoff, M. Karplus, and R. P. Hurst, ibid. 44, 505 (1966).

[11]C. A. Coulson, Trans. Faraday Soc. 33, 1479 (1937).

[12]B. J. Ransil, J. Chem. Phys. 35, 1967 (1961).

[13]S. Wang, Phys. Rev. 31, 579 (1928).

[14]W. Kolos and L. Wolniewicz, J. Chem. Phys. 46, 142 (1967).

[15]E. Clementi, IBM Research Paper RJ-256, August 6, 1963.

[16]D. A. Johnston, C. J. Oudemans, and R. H. Cole, J. Chem. Phys. 33, 1310 (1960).

[17]N. C. Dutta, T. Ishihara, C. Matsubara, and T. P. Das, Phys. Rev. Letters 2, 8 (1969).

[18]E. Fues, Z. Phys. 82, 536 (1933).

[19]B. J. Ransil, Rev. Mod. Phys. 32, 245 (1960).

[20]R. M. Stevens, R. M. Pitzer, and W. N. Lipscomb, J. Chem. Phys. 38, 550 (1963).

[21]S. Huzinaga, ibid. 42, 1293 (1965).

[22]T. H. Dunning, ibid. 53, 2823 (1970).

[23]P. Wynn, Math. Aids Computation 54, 91 (1956); G. A. Petersson and V. McKoy, J. Chem. Phys. 46, 4362 (1967).

[24]A. A. Maryott and F. Buckley, U.S. Natl. Bur. Stds. Circular 537 (1953).

[25]See, for example, T.-K. Lim, B. Linder, and R. A. Kromhout, J. Chem. Phys. 52, 3831 (1970).

[26]J. P. McTague and G. Birnbaum, Phys. Rev. 3A, 1376 (1971).

[27]J. P. McTague, C. H. Lin, T. Gustafson, and R. Chiao, Phys. Letters 32A, 82 (1970).

TABLE I. Polarizability of H_2 for various wavefunctions.

	R	STO Bases $\{\chi^0\}$, $\{\chi^1\}$[a] for Hartree-Fock (HF) or Valence Bond (VB) Wavefunctions	$\alpha_{\parallel}$ (% error)[b]	$\alpha_{\perp}$ (% error)
(A)	1.402	$\{0\}$ = 1s (1.197) HF $\{1\}$ = 2p, 3p (1.197)	6.345 (-1.0)	4.238 (-7.5)
(B)	1.406	$\{0\}$ = 1s (1.166) VB $\{1\}$ = 2p, 3p (1.166)	6.003 (-7.1)	4.441 (-3.4)
(C)		$\{1\}$ = 2p, 3p (1.100)		4.469 (-2.8)
(D)	1.402	$\{0\}$ = 1s (1.378), 2s (1.176) 2p (1.820) HF $\{1\}$ = 2p, 3p (1.378)	6.090 (-4.9)	4.102 (-10.5)
(E)		$\{1\}$ = 2p, 3p (1.378) 2p, 4p (1.176)	6.321 (-1.3)	4.597 (+2.9)

[a] First-order bases are constrained as linear combinations by the solution of Eq. (10). See text.

[b] Error is relative to the accurate theoretical values of Ref. 14. See text. Accurate values of ($\alpha_{\parallel}$, $\alpha_{\perp}$) are (6.407, 4.584) at $\underline{R}$ = 1.402 and (6.460, 4.597) at $\underline{R}$ = 1.406. All values are atomic units (a.u.), $\underline{a_0^3}$.

Appendix I. Orbital Basis Sets and Their Method of Selection

In our perturbation calculations on H_2, He, Li, Be, and LiH using STO's, our choice of polarization functions was guided by Eq. (10) of the paper. This equation establishes the polarization function for any given pure hydrogenic function. The exact solution for z-polarization are described below. Subscripts STO and HO on orbitals mean "Slater-type orbital" and "hydrogenic orbital," respectively; the two differ in the case of nominal 2s form.

$$(A)\quad \chi^0 = (1s)_{STO} = (1s)_{HO} \quad ; n_p = 1$$

$$\chi^1 = \frac{1}{\zeta 3}\left[(2p_z)_{STO} + \sqrt{\frac{15}{8}}\ (3p_z)_{STO}\right]$$

As noted in the text, ζ is the orbital exponent of the χ^0, as well as of all STØ's in χ^1.

$$(B)\quad \chi^0 = (2s)_{STO} = \left[(1s)_{HO} - (2s)_{HO}\right]/\sqrt{3}$$

We assume that the χ^1 for the two HO components add algebraically. There is an additional problem, that $\underline{(2s)_{HO}}$ and $\underline{(2p_z)_{HO}}$ are degenerate; to solve Eq. (10) for χ^1, we must use the linear combinations $\frac{1}{\sqrt{2}}\left[\underline{(2s)_{HO}} \pm \underline{(2p_z)_{HO}}\right]$ appropriate for degenerate perturbation theory. Corresponding first-order energies are $\underline{E}^{(1)} = \mp\ \frac{3}{2\zeta}$. Then we construct $\chi^1_{\underline{2s, HO}}$ as $\frac{1}{\sqrt{2}}\left[\chi^1_{\underline{(2s+2p), HO}} + \chi^1_{\underline{(2s-2p), HO}}\right]$. The result is:

$$\chi^1 = \frac{1}{\zeta^3}\left[\left(1 - \frac{5}{2}\sqrt{3}\right)(2p_z)_{STO} + \sqrt{\frac{15}{8}}\,(3p_z)STO - \frac{3}{2}\sqrt{35}\,(4p_z)_{STO}\right]$$

$$(C)\ \chi^0 = (2p_z)_{STO} = (2p_z)_{HO}$$

Following (B), we construct

$$\chi^1_{\underline{2p_z,\,HO}}\ \text{as}\ \frac{1}{\sqrt{2}}\left[\chi^1_{\underline{(2s+2p),\,HO}} - \chi^1_{\underline{(2s-2p),\,HO}}\right],$$

with the result

$$\chi^1 = \frac{1}{4\zeta^3}\left[(1s)_{STO} - \sqrt{3}\,(2s)_{STO} - \sqrt{\frac{45}{8}}\,(3s)_{STO} + \sqrt{\frac{35}{4}}\,(4s)_{STO}\right]$$

$$- \frac{3}{4\zeta^3}\left[(3d_{3z^2-r^2})_{STO} + \sqrt{\frac{7}{2}}\,(4d_{3z^2-r^2})_{STO}\right]$$

$$(D)\ \chi^0 = (2p_x)_{STO}$$

$$\chi^1 = \frac{1}{\zeta^3}\left[\sqrt{\frac{27}{8}}\,(3d_{xz})_{STO} + \sqrt{\frac{21}{4}}\,(4d_{xz})_{STO}\right]$$

For the $\alpha_{\parallel} = \alpha_{zz}$ calculations on LiH, the constraints of the χ^1 to the above linear combinations were relaxed, and the primitive STO's occuring in the χ^1 were used as individual free basis functions.

For zero-order bases $\{\chi^0\}$ composed of GTO's, the unperturbed reference Hamiltonian for each function is no longer than that of the hydrogenic atom with its coulombic binding potential. It is instead the Hamiltonian for a harmonic oscillator. This is not realistic for the χ^0 as used, so we adopted a different technique of

selecting the χ^1 for nonorthogonal perturbation theory or fully self-consistent calculations. Basically, we referred the total GTO basis to an equivalent STO basis, constructed the corresponding (unconstrained) STO $\{\chi^1\}$, and converted the latter to GTO's. As the first step we examined the range of orbital exponents in the GTO's of any one type on one center, such as 1s on Li in the LiH case. Then we reversed Hurzinaga's (Ref. 20) prescriptions for fitting one STO with n GTO's by energy minimization. For example, Huzinaga reports that four $(1s)_{GTO}$ used to fit one $(1s)_{STO}$ range in exponents ζ_G from 0.123 $(\zeta_S)^2$ through 13.36 $(\zeta_S)^2$. In reversing Huzinaga's procedure, we identify the extreme high and low Gaussian exponents with components in expansions of the two STO's with highest and lowest exponents ζ_S. If the extreme ζ_G are g_1 (low) and g_2, respectively, the corresponding extreme ζ_S are $s_1 = \sqrt{g_1/0.123}$ and $s_2 = \sqrt{g_2/13.36}$. We then assume these two STO's polarize into the familiar STØ χ^1 above, which we reexpress in GTO's. We look at only the GTO χ^1 of extreme exponents and fill in other Gaussians in a geometric progression of exponents, usually with a ratio 3.3. Since the extreme exponents for STO χ^1 are the same as those for the STO χ^0, the conversion is simple. Thus if we are discussing only the 1s types among the GTO χ^0 and have constructed s_1 and s_2 for the corresponding STO (2p) and (3p), we need only choose the conversion of the STO (2p) and (3p) to GTO (2p)[GTO (3p) exist but are harder to use in integral routines]. Using four $(2p)_{GTO}$ to convert one $(2p)_{STO}$, the $(2p)_{GTO}$ range in exponents from 0.020 $(2s_1)^2$ to 0.734 $(2s_2)^2$.

For our fully self-consistent calculations, $\{\chi^0\}$ and $\{\chi^1\}$ combine into one large set. The zero-order basis was chosen first, and then augmented by $\{\chi^1\}$ chosen as above, deleting any χ^1 which were redundant, or nearly so, with any of the χ^0. The zero-order GTO basis for LiH was chosen in correspondence to the STO basis used by Ransil (Ref. 18), again by finding the extremes in exponent range for the corresponding GTO's and filling in with a geometric progression. This procedure has some drawbacks relative to good exponent optimization, drawbacks not remedied simply by adding a few more basis functions. Lack of closely spaced exponents is one difficulty, as it disallows generation of more diffusive atomic orbitals with radial nodes. At the high exponent end the lack of optimization incurs a penalty in zero-order energy, plus a slight unbalancing of the basis set. By trial and error we adjusted the total basis for LiH, adding and deleting functions at the extremes of the exponent range for each symmetry type and center--we even added a $\underline{(1s)}_{GTO}$ in the middle of the range to form a close-exponent pair, and we contracted the tightest $\underline{(1s)}$ functions on each center into one function. These trials and their resulting α values are recounted shortly.

For N_2 we began with Dunning's zero-order basis (Ref. 21) consisting of 44 primitive GTO's contracted into 26 functions. On the basis of our experience with LiH, we added one more diffuse function of each type $\underline{(1s)}$, $\underline{(2p_x)}$, $\underline{(2p_y)}$, $\underline{(2p_z)}$ on each center. The extra $\underline{(2p)}$ represent polarization of $\underline{(1s)}$ types, and the extra $\underline{(1s)}$ functions represent part of the χ^1 for the zero-order $\underline{(2p)}$. We also

added 5 types of $\underline{(3d)_{GTO}}$ on each center to represent the rest of the χ^1 for the zero-order (2p). Careful selection of polarization functions for the zero-order (2p) forming the diffuse and very polarizable π orbitals is most important. The rationale for each type of $\underline{(3d)_{GTO}}$ is given in the paper. Four of the basic symmetry types XX, YY, ZZ, and XY occur in only one of the two possible linear combinations because the other combination does not represent the first-order polarization of any occupied molecular orbital.

Complete Specifications on Basis Sets

The second entry in each set is the type of calculation done--'OPT' for orthogonal perturbation theory, 'NOPT' for non-orthogonal perturbation theory, and 'FSC F' for fully-self-consistent-field. The H_2 bases are given in Table I in the paper and are not reproduced here.

He

α = 1.319 OPT $\{0\}_{STO}$ = 1s (1.44608), 2s (2.86222)
E. Clementi, IBM Research Paper RJ-256, August 6, 1963.
$\{1\}_{STO}$ = 2p, 3p (1.44608, 2.86222)--constrained linear combinations in χ^1

Li

α = 167.6 OPT $\{0\}_{STO}$ = 1s (2.43309, 4.51769) } restricted
2s (0.67142, 1.97812) } Hartree-Fock
E. Clementi, op. cit.
$\{1\}_{STO}$ = 2p (2.43309, 4.51769)
2p, 3p (0.67142, 1.97812)--constrained linear combinations in χ^1

Be

α = 45.28 OPT $\{0\}_{STO}$ = 1s (3.3370, 5.5063)
2s (0.6040, 1.0118)
E. Clementi, op. cit.
$\{1\}_{STO}$ = 2p (3.3370, 5.5063)
2p, 3p (0.6040, 1.0118)--constrained linear combinations in χ^1

LiH (STO)

various trials
$R = 3.015$ a.u. $= R_e$

$\{0\}$ = Li: 1s (2.6909), 2s (0.7075), $2p_z$ (0.8449)
H: 1s (0.9766)
B. J. Ransil, Rev. Mod. Phys. 32, 245 (1960).

$\alpha_\perp = 26.22$ OPT

$\{1\}$ = Li: $2p_x, 3p_x$ (2.6909, 0.7075), $4p_x$ (0.7075),
$3d_{xz}, 4d_{xz}$ (0.8449)
H: $2p_x, 3p_x$ (0.9766)
-constrained linear combination in χ^1

19.49 OPT

$\{1\}$ = as above, less Li: $3p_x$ (2.6909), H: $2p_x$ (0.9766)
-constrained linear combinations in χ^1;
constraint is probable cause of much poorer α

$\alpha_\parallel = 25.29$ NOPT

$\{1\}$ = Li: $2p_z, 3p_z$ (2.6909, 0.7075), $4p_z$ (0.7075),
$1s, 2s, 3s, 4s, 3d_{3z^2-r^2}, 4d_{3z^2-r^2}$ (0.8449)
H: $2p_z, 3p_z$ (0.9766)
-all unconstrained

we will use here.

*: contracted, with coefficients 0.726440, 0.292317, 0.060146, 0.002333.

**: contracted, with coefficients 0.763697, 0.249790, 0.056681, 0.010246.

$\alpha_{\parallel}$ = 22.78

E_0 = -7.9832

μ_0 = 2.3567

V/T = 2.00062

Li-1s: 0.033, 0.110, 0.360, 1.20, [4.00-330.0]

$2p_z$: 0.0080, 0.0264, 0.0871, 0.290, 0.960, 3.20

$3d_{z^2}$: 0.018, 0.200

$3d_{x^2}$, $3d_{y^2}$: 0.060

H-1s: 0.080, 0.0264, [0.871-58.0]

$2p_z$: 0.018, 0.200, 0.660

Supposed "best set," deleting functions from above set which contributed least polarization: 21(27)

$\alpha_{\parallel}$ = 22.36

E_0 = -7.9835

μ_0 = 2.3568

V/T = 2.00118

Li-1s: 0.010, 0.033, 0.110, 0.360, 1.20, [4.00-330.0]

$2p_z$: 0.0264, 0.0871, 0.290, 0.960

$3d_{x^2}$, $3d_{y^2}$, $3d_{z^2}$: 0.060, 0.200, 0.660

H-1s: 0.024, 0.080, 0.264 [0.871-58.0]

$2p_z$: 0.018, 0.060, 0.200, 0.660

"Best big set" after more experience in tailoring the first GTO set: 27(33); probably best balanced in both orders.

$\alpha_{\|}$ = 21.74

E_0 = -7.9830
μ_0 = 2.3608
V/T = 2.0067

Li-1s: 0.033, 0.110, 0.360, 1.20 [4.00-330.0]
$2p_z$: 0.0871, 0.290, 0.960
$3d_{x^2}, 3d_{y^2}, 3d_{z^2}$: 0.200
H-1s: 0.024, 0.080, 0.264, [0.871-58.0]
$2p_z$: 0.060, 0.200

Cutting all minor contributors from above set: 17(23)

$\alpha_{\|}$ = 21.06

Li-1s: 0.033, 0.110, 0.200, 0.360, 1.20, [4.00-330.0]
$2p_z$: 0.0871, 0.290, 0.960
H-1s: 0.024, 0.080, 0.264, [0.871-58.0]
$2p_z$: 0.200

Simplest "adequate" basis for $\alpha_{\|}$: 14(20)

$\alpha_\perp = 22.56$

Li-1s: 0.033, 0.110, 0.200, 0.360, 1.20, [4.00-330.0]
$2p_z$: 0.290, 0.960
$2p_x$: 0.0871, 0.290
H-1s: 0.024, 0.080, 0.264, [0.871-58.0]
$2p_z$: 0.200
$2p_x$: 0.080, 0.200

Simplest "adequate" basis for $\alpha_\perp$: 17(23); it is obvious how to combine this with the above set to get the best total basis - which we did not waste time doing, instead proceeding to N_2.

N_2 GTO

$\underline{R} = 2.068$ a.u. $= \underline{R_e}$

Zero-order basis functions from Dunning's N_2 wavefunction (Ref. 22) are unmarked. Polarization functions we added are starred. Basis functions occurring free on each center are denoted as $(\ )_{\underline{A}}$, $(\ )_{\underline{B}}$; those occurring on both centers but constrained to only one of the two linear combinations are denoted as $(\ )_{\underline{A}} \pm (\ )_{\underline{B}}$. Total basis is 40(66) GTO's.

				coefficients (from Dunning)
$\alpha_{\parallel} = 14.97$	$1s_A, 1s_B$	5909.4399	contracted	0.0020033
$\alpha_{\perp} = 9.464$		887.4510		0.0153045
		204.7490		0.0742662
$E_0 = -108.89926$‡		59.8376		0.2532725
$V/T = 2.00054$		19.9981		0.6003592
		2.6860		0.2450225
		7.1927		
		0.7000		
		0.2133		
		0.0800*		
	$2p_{x_A}, 2p_{x_B}, 2p_{y_A}, 2p_{y_B}, 2p_{z_A}, 2p_{z_B}$	26.7860	contracted†	0.0267996
		5.9563		0.1708759
		1.7074		0.5726499
		0.5314		
		0.1654		
		0.0800*		
	3d: $XX_A + XX_B$	0.200*		
	$YY_A + YY_B$	0.200*		
	$XY_A + XY_B$	0.200*		
	XZ_A	0.200*		
	XZ_B	0.200*		
	$YZ_A + YZ_B$	0.200*		

†Originally, the 2p function of exponent 0.5314 was included in a four-way contraction. We split if off for polarization freedom.

‡Compare to Dunning's zero-order values, $E_0 = -108.8877$.

Appendix II. Extended Comments on the Derivation and Use of Nonorthogonal (Hartree-Fock) Perturbation Theory

We mentioned in the paper that the nonorthogonal perturbation theory (NOPT) as given by Das and Duff eventually caused us problems. Their formalism uses the approximation that the zero-order Hartree-Fock equation

$$(h^0 - \epsilon_i^0)u_i^0 = 0 \tag{A}$$

is exactly satisfied: in projecting with any function χ_p^1 we obtain zero

$$\langle \chi_p^1 | h^0 - \epsilon_i^0 | u_i^0 \rangle = 0 \tag{B}$$

Actually, if the basis $\{\chi^1\}$ contains any functions not in $\{\chi^0\}$, then Eq. (B) is not true. We recount here our findings in trying to derive the most exact NOPT equations and to use them.

There are two basic expressions which any NOPT formalism must yield. First and more important is the first-order Hartree-Fock equation satisfied by the nonorthogonal (in first order) orbitals. Expansion of the first-order orbitals $\underline{u_i^1}$ in the first-order basis $\{\chi_p^1\}$

$$u_i^1 = \sum c_{ip}^1 \chi_p^1, \tag{C}$$

and projections of the first-order equation with each χ_p^1 in turn

yield linear equations for the c^1_{ip}. The second expression needed from NOPT is that for the second-order energy $E^{(2)}$ of the total determinantal Hartree-Fock wavefunction--simplified by use of the first-order differential equation (1.d.e.) to a form involving only matrix elements of the perturbation operator h^1 (in orthogonal Hartree-Fock [OHF] the expression is simply

$$E^{(2)} = \sum_i \langle u^0_i | h^1 | u^1_i \rangle). \tag{D}$$

The general route to the 1.d.e. of NOPT is to construct the total energy $\langle E \rangle$ for the wavefunction through second order (in any one orbital consider only terms through first order in non-orthogonality); perform the variation of the energy with respect to u^1_i, $\delta E/\delta u^1_i$, and select the first-order part; and finally simplify as much as possible with use of the zero-order differential equation (0.d.e.)--preferably only in its exact form

$$\langle u^0_j | h^0 - \epsilon^0_i | u^0_i \rangle = 0 \tag{E}$$

and not assuming additionally the validity of Eq. (B). For practical calculations the 1.d.e. is converted to linear equations for the u^1_i expansion coefficients in the basis $\{\chi^1\}$. Before any numerical work, it is valuable to check the linear equations at least for symmetry: the linear equations from the 1.d.e. have the form

$$F_{ip;jq}\, c_{jq} = I_{ip} \tag{F}$$

where the (ip)-th equation comes from the variation $\underline{\delta E/\delta u_i^1} = 0$ projected with χ_p^1. We require

$$F_{ip;jq} = F_{jq;ip} \tag{G}$$

since

$$F_{ip;jq} = \frac{\partial}{\partial c_{jq}} \left(\frac{\partial E}{\partial c_{ip}} \right) = \frac{\partial^2 E}{\partial c_{jq} c_{ip}} \tag{H}$$

and

$$F_{jq;ip} = \frac{\partial^2 E}{\partial c_{ip} \partial c_{jq}} \tag{I}$$

and the order of derivatives cannot matter because the energy $\underline{E}$ is analytic in the coefficients (particularly because the coefficients contain the electric field strength).

Das and Duff follow the three-part route described above. Their Eq. (7) is the Hartree-Fock expectation value of the energy, through second-order. Their Eq. (10) is the result of the variation $\underline{\partial E/\partial u_i}$ after using the 0.d.e. [in the extended, approximate sense of Eq. (B)] to simplify it. It is still of mixed orders, zero through two, but the first-order terms are at their simplest. Thus they have done the last two steps at once in going from their Eq. (7) to Eq. (10). Finally, they explicitly select the first-order part of their Eq. (10), displaying the zero- and first-order parts of the one-electron operator, $\underline{h^0}$ and $\underline{h^1}$, explicitly also; the result is Eq. (14).

Our attempts to use NOPT as given by Das and Duff (DD) began with a derivation of the form appropriate to doubly-occupied molecular orbitals. We worked from the OHF equations (12) adapted to double occupancy by the simple expedient of interpreting the operation $\langle a|\cdot|b\rangle c$ as

$$2\langle a(1)|g_{12}|b(1)\rangle c(2) - \langle a(1)|g_{12}|c(1)\rangle b(2) \qquad (J)$$

rather than as in Appendix I. After symmetric deorthogonalization of the orthogonal orbitals $\bar{u}_i$ as

$$\bar{u}_i = u_i - \tfrac{1}{2}\sum_{k\neq i} \langle u_k|u_i\rangle u_k, \qquad (K)$$

we obtained a first-order equation not in entire analogy to Eq. (14), but by using the assumption of Eq. (A) three times we completed the analogy. The lack of rigor for Eq. (14) or its double-occupancy analog was somewhat disturbing but initially felt to be of the same or lesser order than the inherent error in finite-basis expansion of orbitals.

Our second step was checking the symmetry of the linear equations derived from our analog of Eq. (14), that is, the satisfaction of Eq. (G). We found an asymmetry, though it could be removed by removing a summation restriction $k \neq j$ appearing in Eq. (14) or its analog. After correspondence with both Das and Duff, we confirmed our interpretation of some ambiguous terms in Eq. (14) and resolved our original problem as one of convention.

To eliminate possible ambiguity in the deorthogonalization prescription, Eq. (K) or their Eq. (11), the restriction

$$\langle u_i^1 | u_i^0 \rangle = 0 \qquad \text{(L)}$$

was entered. This auxiliary condition must be incorporated into the linear equations (F) for the c_{ip}^1 as extra equations [and then (G) need not hold], or it can be incorporated after the solution. That is, the orbitals u_i^1 and

$$u_i^1 = u_i^1 - \langle u_i^1 | u_i^0 \rangle u_i^0$$

satisfy the same 1.d.e. Thus in principle we could drop the summation restriction as we had planned (the added term vanishes anyway).

We derived the expression for $E^{(2)}$ at this time, both by deorthogonalizing the total Hartree-Fock energy and projecting second-order terms, and by direct deorthogonalization of the simplified $E^{(2)}$. Both times we found the result

$$E^{(2)} = \sum_i \{\langle u_i^0 | h^1 | u_i^1 \rangle - \sum_{j \neq i} \langle u_i | u_j \rangle' \langle u_i^0 | h^1 | u_j^0 \rangle\}, \qquad \text{(M)}$$

where

$$\langle u_i | u_j \rangle' = \langle u_i^1 | u_j^0 \rangle + \langle u_i^0 | u_j^1 \rangle,$$

and the restriction $j \neq i$ applies when $\langle u_i^0 | u_i^1 \rangle = 0$ is forced. As a check, we programmed OHF PT to compare to NOPT using the

unoccupied virtual orbitals as the $\{\chi^1\}$. We also verified that Eq. (14) correctly reduces to OHF PT.

As we noted in the paper, our initial numerical results showed much instability in the calculated second-order energy with regard to basis changes. Some instability was probably due to using Eq. (M) with the restriction $i \neq j$ intact, but some remained after removing the restriction. Apparently the use of assumption (A) was responsible.

Quite a while later, we attempted a derivation of the most correct 1.d.e. We deorthogonalized the OHF equations with the extra $k = i$ term in the deorthogonalization. We found that the 0.d.e. is used in both stages of Das and Duff's derivation, going from Eq. (7) → Eq. (10) and from Eq. (10) → Eq. (14). In our more correct analog to Eq. (14), derived without use of the 0.d.e. and also allowing $\langle u_i^0 | u_i^1 \rangle \neq 0$, we found the linear equations it gave were not symmetric. Yet the use of the 0.d.e. to derive Das and Duff's Eq. (14) valid for $\langle u_i^0 | u_i^1 \rangle \neq 0$ did yield symmetric linear equations. The symmetry should be unaffected by use of the 0.d.e. This paradox is yet unresolved, after much rechecking of algebra.

Starting afresh, we took Eq. (7) (which we assumed was accurate) and projected $E^{(2)}$ explicitly from it. We then performed the variation $\delta E^{(2)}/\delta u_i = 0$ to get the 1.d.e. Some summation restrictions had to be cleared up and then we obtained symmetric linear equations. However, the numerical results were unstable

as before. A check of Eq. (7) was initiated, deriving the expectation of the energy E through second order by directly calculating the contributions of each permutation operator in the matrix elements $\langle\psi|\underline{H}|\underline{A}\psi\rangle$, $\langle\psi|\underline{A}\psi\rangle$ where ψ is the unsymmetrized straight product of HF orbitals, $\underline{A}$ is the familiar antisymmetrizer composed of a sum of signed n-electron permutations, and $\underline{H}$ is the total N-electron Hamiltonian. The 1.d.e. we derived by variation contained new terms and, unfortunately, did not reduce to Eq. (14) under the assumptions of Eqs. (A) and (L) [yet Eq. (14) is known to be the valid deorthogonalized form of the OHF equations under these assumptions, as we showed before].

In sum, our problems are twofold: the inability to verify Eq. (7) for the total energy either (1) by reference to the more basic form $\underline{E} = \langle\psi|\underline{H}|\underline{A}\psi\rangle/\langle\psi|\underline{A}\psi\rangle$ or (2) by exact reduction of Eq. (7) to a symmetric, stable set of linear equations. Amplifying the latter problem, we note that avoiding use of the 0.d.e. should preserve the variational principle for $\underline{E^{(2)}}$ with respect to the basis $\{\chi^1\}$, independent of any errors in (A) from finitude of the basis expansion. That is, the numerical results should be stable and $E^{(2)}$ monotonic with addition of χ^1 functions.

Soon after encountering all these difficulties, we abandoned NOPT for the equivalent FSCF approach, achieving acceptable results for both LiH and N_2. The proper NOPT equations still elude us, but we feel they are not as useful or reliable as FSCF, contrary to our original estimations. We now cover the exact

utilities of OPT, NOPT, and FSCF approaches to sustain this last claim.

Given a zero-order basis $\{\chi^0\}$, the best bases $\{\chi^1\}_x$ and $\{\chi^1\}_z$ for the two directions of polarization are well-defined in our scheme. The two straightforward ways of proceeding to calculate $\underline{E^{(2)}}$ and α are OPT and FSCF. In both we combine all three bases into one large basis, eliminating redundant functions, and obtain a set about twice as large as $\{\chi^0\}$ for small molecules, or perhaps 1.5 times as large for big molecules (N_2). Of course, we combined both $\{\chi^1\}$ at once to avoid unbalancing the two calculations, $\alpha_{\underline{xx}}$ and $\alpha_{\underline{zz}}$, and lowering the anisotropy accuracy thereby. The two-electron integral computation time is 16 down to 5 times that for $\{\chi^0\}$, depending on molecular complexity. OPT and FSCF give equivalent results in this total basis. [While FSCF is more readily adapted from existing SCF programs, OPT can be faster in the actual 1.d.e. solution if we borrow the complicated integral-handling from SCF programs.] The nonstraightforward procedure is NOPT, requiring two separate basis set mergers, $\{\chi^0\} + \{\chi^1\}_x$ and $\{\chi^0\} + \{\chi^1\}_z$, again eliminating redundant functions. The merged sets are roughly 1.6-1.35 times as large as $\{\chi^0\}$ [small and large molecule limits], and require total two-electron integral times range from 13-6.6 times that for $\{\chi^0\}$. The total calculation time for NOPT is only trivially smaller than that for OPT or FSCF--yet NOPT is so much harder to obtain in correct form, and in addition its α calculations do not give the

zero-order MO determination the benefit of using the diffuse polarization functions to increase the accuracy (of the zero-order MO's, hence also of α itself).

Introduction

Utility of Vibrational Energy Transfer Studies in Chemistry

The problem of molecular vibrational or rotational excitation in binary collisions is well studied, perhaps overly so in some respects. Many different kinds of experiments in thermal, hot-atom, or molecular beam systems are aimed at extracting vibrational (or less often, rotational) excitation cross-sections or relaxation times, especially for the lower energy levels which are easiest to distinguish individually. In addition there have been many calculations on simplified models of the colliding molecules, quantum and classical, exact and approximate. We present such a model calculation for the H_2-H_2 system in a paper following this introduction.

The understanding of vibrational relaxation in particular is important for chemistry. It is deeply involved in collisional activation[1] in gas reactions, and it is also of interest for other bulk processes: ultrasonic absorption and other transport (see the introduction to part I of this thesis); optical fluorescence[2] (including the existence of competing radiationless decay[3] in large molecules), and molecular laser operation[4]; and some esoteric astrophysical processes[5], such as comet tails and nebular radio emission. As chemists, we concentrate on its importance in the theoretical understanding of chemical reactions.

A chemical description of a bulk system in terms

of singlet distribution functions (concentrations) for distinct molecular species is presumably accurate for thermodynamic, transport, electromagnetic, and other macroscopic properties. (The neglected 'physical' interactions of molecules cause severe problems in dense phases, of course--see the introduction to part I of this thesis, especially section G on associated liquids.) With this presumed to be true, the change of system properties (including heat, work) with time is ascribed to changes in concentration of chemical species[6] through reactions.

In any complex kinetic system in bulk matter, it is reasonable to assume we can decompose the rates of change of species concentrations and corresponding bulk properties into elementary steps or reactions. Each elementary reaction is taken as a simple rate process described by a rate law, with the rate constant dependent on temperature, pressure, and other conditions (and only weakly on chemical composition). Of course for nonthermal systems this is a more questionable analysis and a direct appeal should be made to time-dependent molecular distribution functions or other essentially complete many-body descriptions--and even in fast-reacting thermal systems the local and transient disturbances from local thermodynamic equilibrium require corrections to the forms of empirical rate law expressions[7]. To continue, this principle of decomposability into elementary reactions is the foundation of all chemical kinetics.

Let us consider the molecular dynamics and some of the statistical-mechanical nature of the binary collisions in the various kinds of elementary reactions, particularly regarding the role of vibrational energy. For brevity we must omit discussion of the often fascinating coupling[8] of elementary steps into total reacting systems, involving staging, competition, branching, and elegant derivative phenomena such as feedback loops common in biochemistry[9].

All types of elementary reactions are presumably governed by the same general laws of quantum mechanics and statistical mechanics. However, a real understanding demands detailed (and necessarily approximate or modeled) theoretical frameworks and experimental techniques, very much dependent on the specific type of reaction. After all, chemical reactions range from ionic solid reactions through aqueous acid-base reactions and electrochemistry to free-radical gas phase reactions. Reactions may be classified by MOLECULARITY: unimolecular, bimolecular, (rarer) termolecular and higher. In the interest of unity, we may claim that unimolecular reactions are a limiting case of bimolecular ones, with a metastable, unarranged product in the reactive region of molecular configuration,or arrangement channel. Similarly, termolecular recombinations are viewed as the inverse of bimolecular dissociation, which is reaction into a new arrangement channel above an energetic threshhold. REARRANGEMENT TYPE is another division scheme on the basis

of the exact manner of particle regrouping: exchange (atom or group), abstraction, simple charge transfer; recombination/dissociation (for termolecular only). The ELECTRONIC FORM OF REACTANTS, whether ionic, neutral, or free radical, influences the gross nature of the intermolecular interaction potential. The manner of ENERGIZATION or initiation determines the relative involvment of the various molecular degrees of freedom (d.o.f.) and the statistics governing energy transfer among them both temporally and spatially: thermal--all d.o.f.; photochemical or (particle-)radiative = hot-atom--variable balance of translation, vibration, chiefly; shock wave--translation initially; molecular beam (non-bulk)--any desired d.o.f. or combination, in principle. The THERMODYNAMIC STATE or STATE OF AGGREGATION is a chief determinant of the statistics of energy and mass redistribution in <u>successive</u> collisions: dilute gas, dense fluid, solid; pure, diluted by inert species, solvated; homophase or heterophase situation of reaction partners. Changes of phase from reactants to products (e.g., precipitation, gas evolution) affect the kinetics on the hydrodynamic time scale (much longer). Catalysis is challenging to describe theoretically, as it involves a special aggregation or three-body-level molecular distribution, often heterophase. The MODE OF PROPAGATION is rather like a subset of rearrangement type: chain, branched, nonchain; polymerizing or not. Special aspects of propagation such as caging[10] in

liquids could be added here, or under the thermodynamics; caging is a result of significant structure in the two-body molecular distribution functions and their time-evolution. THERMODYNAMIC CONSTRAINTS in the bulk (adiabatic, isochoric, or isobaric maintenance; openness to mass exchange; hydrodynamic conditions of flow or mixing; and phase change during reaction) give convenient further divisions but are not essential either empirically or microscopically. Such constraints are merely boundary conditions on the differential equations of species, momentum, and energy balances already fixed by the basic rate laws.

The eventual goal of experimental or theoretical reaction studies is extraction or calculation of the rate law, including its dependence on temperature, pressure, etc. and also its dependence on a few basic features of the molecules. More detailed information is possible, especially theoretically (which may be viewed as a more fundamental approach to the temperature dependence, etc.): rate constants in rate laws are simple thermal (Boltzmann) averages of more basic reactive cross-sections[11]. If the relative translational energy $\underline{E}$ of the reactants in a given encounter is a valid total delineation for the collision (other d.o.f. are presumed to have a Boltzmann population of their energy levels at some temperature low compared to the equivalent translational temperature--often true for the important range of translational energy), then a cross-section $\sigma(\underline{E})$ is

a more detailed result[11]. For complete state resolution in reactants and products of all d.o.f. energy levels, the result is $\sigma(\underline{n},\underline{m})$, where $\underline{n}$, $\underline{m}$ denote the complete set of quantum numbers for the reactants, products. More quantum-mechanically correct is the S-matrix $\underline{S}(\underline{n},\underline{m})$ $\sigma = |S|^2$, for proper compounding of multi-stage processes of activation.

The problem we address in our vibrational excitation studies is, How does vibrational energy storage and transfer affect the equilibria and rates for each type of reaction above? There is sketchy knowledge for limited types of reactions. Unimolecular decomposition rates of gases are apparently well-explained[12] by the accumulation of large amounts of vibrational energy in all the molecular bonds through hard collisions. The actual decomposition occurs when by chance most of the quanta localize in one bond and break it. The theory has seen many successive refinements. Simple gas-phase abstraction reactions, such as K + HCl-- KCl + H, are also undergoing much study[13]. Polanyi[14] in particular has sought the effects of very general features in the potential energy surface (on which the reactants and products move; see later) on the effectiveness of reactant vibrational energy in causing reaction, or conversely, on the degree of vibrational excitation in the products. Some qualitative knowledge has been gained in this regard about attractivenss or repulsiveness of entrance and exit channels, presence of net energetic barriers either

direction (endo- or exo-thermicity of reaction), and entrance or exit location of additional, local energetic barriers or wells. Finally, vibrational energy flow is readily followed in systems fitting the stochastic[15] (strong collision, totally diabatic) or transition-state[16] (completely adiabatic) models, which apply in rare limiting cases but then among almost all classes of reaction. In the stochastic model all energy in the reactants (and products, as well) is equivalent. In transition-state theory, the change of vibrational quantization from reactant to intermediate and on to product transfers definite amounts of energy to other degrees of freedom, to retain adiabaticity in every d.o.f.

Most reactions fall outside the scope of the reaction classes and theoretical models above, and require more detailed analysis and calculations in order to understand the absolute rates and their dependence on thermodynamic conditions and molecular structure. Beginning with the surer knowledge of the statics--of the vibrational level spacing/density in all the important reactant configurations, we must develop the dynamics: the coupling of the vibrational d.o.f. to other d.o.f. in collisions, and how collisions compound statistically in succession. Some averaging procedure for the d.o.f. not directly involved in reaction must also be developed. Theoretical studies are generally of two types: (1) a' priori models of the molecular

dynamics, proceeding from many cross-section calculations over representative energy ranges and partner orientations (classically--over translational and internal states, quantum-mechanically) to a final macroscopic rate constant; (2) fitting experimental rate constants to a parametric form of the cross-section as $\sigma(\underline{E})$ [11], assuming a model in which $\underline{E}$ = relative translational energy is all that matters. The latter is a more recent approach. The former is more basic and even underpins the latter, and thus we concentrate on it.

Let us consider the general approach to the theory of reactions through collision dynamics (scattering theory), particularly for 'clean' gas-phase bimolecular reactions. A model is selected for the division of the internal molecular d.o.f., and the reaction coordinates identified along with the proper division of configuration space into reactants, products, and interaction region. One then assumes a potential energy surface (PES) for the total molecular motion (from molecular quantum mechanics calculations generally--fraught with its own great difficulties[5,17]) and projects it onto the reaction coordinates as a cut in the hyperspace of total motion; the potential variation in the remaining d.o.f. coordinates is developed as some basis expansion, usually. One might also assume directly the form of the PES projection on the reaction coordinate and main d.o.f., commonly a Lennard-Jones analytic form in some key interatomic coordinate. The Hamiltonian for the equations of motion must

be simplified to involve only the reaction coordinate and a few important d.o.f.; other d.o.f. are neglected, or rarely, averaged analytically or approximately. In the d.o.f. remaining explicitly, one then distinguishes the 'channels' or net quantum states of motion, as by relative kinetic energy $\underline{E}$, total angular momentum $\underline{J}$, vibrational quantum numbers $\underline{n_i}$ --often neglecting subdivision into rotational states. The blocks of channels which are coupled by the potential are identified. For example, channels of different total $\underline{J}$ do not couple; the total wavefunction or classical phase-space distribution breaks into a sum over various $\underline{J}$-components, called partial waves in quantum mechanics[18]. The differential equations(d.e.) of motion are solved for the whole relevant range of initial conditions (initial channels) with proper scattering boundary conditions imposed[19,20]. Either quantum or classical (or semiclassical) equations can be assumed, and then solved by essentially exact or else approximate (perturbation, variation) methods.

In the quantum treatments of the related inelastic but nonreactive scattering, one invariably performs a channel expansion of the total wavefunction for the motion (in a stationary state representation). Extra channels are included which are not energetically accessible at long times ('virtuals'; their involvement in motion generates some uniquely quantum phenomena--tunneling[21] through classical barriers; and resonances[22] which are rapid changes, with

initial energy, of the exit channel distribution, from rapid alteration in quantum interference effects). The total Schrodinger d.e. factors into coupled d.e.'s for the channels. Solution methods for the CC equations vary widely[23] in approach and in adaptability to different probelms. Returning to reactive scattering, we encounter difficulties in channel expansions because the channels of one arrangement channel are a complete set, yet boundary conditions in the other arrangement channels (products, e.g.) cannot be formulated in terms of them. Physicists[29] attacked this problem first; now there are numerous ways around the problem in a practical sense[20].

Finally the solutions for motion under 'pure' initial conditions are converted to S-matrix elements or scattering cross-sections σ, and then averaged over the (thermal, Boltzmann) statistical distribution in initial channels. Statistical mechanical and quantum corrections for interference among channels or temporally enter here--e.g., corrections for generation of nonequilibrium fluid structure (hence collision statistics) by temporal heating[7] in fast reactions; or corrections for multiple collisions during 'activation' in dense fluids.

We have outlined above an essentially complete, detailed theory. It rarely gets tested in total by actual numerical calculations even without thermal averaging, for realistic systems. Only one total calculation[30] has been

done, in the simplest system $H + H_2 \text{ -- } H_2 + H$ for a few initial kinetic energies. The more practical and valuable use of the theory involves only parts of it at a time, with further simplifications of the equations of motion through models for the coupled molecular motions--even to very crude models such as stripping and harpooning[31], ignoring the detailed internal motions and postulating abrupt shifts in the PES, and using simple gas kinetic theory for total collision (reactive and non-reactive) cross-sections. With sufficient work on models of all degrees of rigor we should hope to develop a manageably small set of concepts to analyze any reaction rate and/or its component cross-sections--or partial aspects of same, such as the effect of simultaneous rotational transitions[32] on vibrational transition cross-sections. An exploding volume of kinetic data and other experimental data (ultrasonic relaxation, laser operation, etc., as noted earlier) is awaiting understanding through correlation with a few basic molecular parameters by use of the theory.

References

1. B. Stevens, Collisional Activation in Gases (Pergamon, Oxford, 1967).

2. See, for example, the review by R. G. Gordon, W. Klemperer, and J. I. Steinfeld, Ann. Rev. Phys. Chem. 19, 215(1968).

3. B. R. Henry and M. Kasha, ibid. 19,161(1968).

4. See refs. 143-149 in review, ref. 2 above; and ref. 116 in the introduction to part I of this thesis.

5. M. Krauss, in Proceedings of the Conference on Potential Energy Surfaces in Chemistry, ed. W. A. Lester, Jr., IBM Publ. RA-18, Jan. 14, 1971, p.6.

6. S. Golden, Quantum Statistical Foundations of Chemical Kinetics (Oxford, 1969).

7. See, for example, W. G. Valance and E. W. Schlag, J. Chem. Phys. 45,4280(1966); N. S. Snider and J. Ross, ibid. 44,1087(1966); R. Kapral, S. Hudson, and J. Ross, ibid. 53,4387(1970); B. Shizgal and M. Karplus, ibid. 52,4262(1970).

8. K. J. Laidler, Chemical Kinetics (McGraw-Hill, N. Y., 1965), Chs. 7,8; S. W. Benson, The Foundations of Chemical Kinetics (McGraw-Hill, N. Y., 1960), Chs. 10, 11.

9. A. L. Lehninger, Biochemistry (Worth, N. Y., 1970), Ch. 8; J. Paul, Cell Biology (Stanford U. Press, Stanford, Calif., 1964), Ch. 7; M. Calvin, Chemical Evolution (Oxford, 1969), Ch. 8.

10. J. Franck and E. Rabinovitch, Trans. Far. Soc. 30,120 (1934); Laidler, op. cit.; Benson, op. cit. ; and many recent references for particular systems.

11. L. A. Melton and R. G. Gordon, J. Chem. Phys. 51,5449 (1969); A. Kuppermann and J. M. White, ibid. 44,4352 (1966); with D. R. Davis and J. A. Betts, to be publ.; A. Kuppermann, J. Stevenson, and P. O'Keefe, Disc. Far. Soc. 44,46(1967).

12. N. B. Slater, Theory of Unimolecular Reactions (Cornell U. Press, Ithaca, N. Y., 1959); and references cited therein; Benson, op. cit.; F. H. Mies, J. Chem. Phys. 51,798(1969); C. W. Larson and B. S. Rabinovitch,

ibid. 51,2293(1969).

13. N. S. Snider, ibid. 51,4075(1969); S. F. Fischer. G. L. Hofacker, and R. Seiler, ibid. 51,3951(1969); D. G. Truhlar and A. Kuppermann, ibid. 52,384(1970); K. T. Tang and M. Karplus, ibid. 49,1676(1968); L. M. Raff, L. B. Sims, D. L. Thompson, and R. N. Porter, ibid. 53,1606(1970); L. L. Poulsen, ibid. 53,1987(1970).

14. J. C. Polanyi, IBM Publ. RA-18, Jan. 14, 1971; and references cited therein.

15. P. Pechukas, J. C. Light, and C. Rankin, ibid. 44,794 (1966), and work cited therein; D. G. Truhlar, ibid. 51,4617(1969); K. Morokuma, B. C. Eu, and M. Karplus, ibid. 51,5193(1969); W. H. Miller, ibid. 52,543(1970).

16. D. L. Bunker, Theory of Elementary Gas Reaction Rates (Pergamon, Oxford, 1966); H. S. Johnston, Gas Phase Reaction Rate Theory (Ronald, N. Y.,1966); D. G. Truhlar, J. Chem. Phys. 53,2041(1970), and references therein; Benson, op. cit.; Laidler, op. cit.

17. A. C. Wahl, IBM Publ. RA-18, Jan. 14, 1971, p. 83; A. D. McLean, ibid., 87.

18. See, for example, N. F. Mott and H. S. W. Massey, The Theory of Atomic Collisions (Oxford, 1965).

19. See our paper following this introduction,for inelastic nonreactive scattering.

20. For reactive scattering. K. T. Tang, B. Kleinman, and M. Karplus, J. Chem. Phys. 50,1119(1969); D. J. Diestler, ibid. 50,4746(1969); T. G. Efimenko, B. N. Zakhariev, and V. P. Zhigunov, Ann. Phys. 47,275(1968); C. C. Rankin and J. C. Light, J. Chem. Phys. 51,1701 (1969); R. A. Marcus, ibid. 49,2610,2617(1968); W. H. Miller, ibid. 50,407(1960).

21. Bunker, op. cit., §2.4.

22. R. D. Levine, B. R. Johnson, J. T. Muckerman, and R. B. Phys. 49,56(1968).

23. The Born, distorted wave, and perturbed stationary state methods (18) are very approximate reductions of the channel coupling; the largely uncoupled CC equations resulting are then numerically integrated by a simple technique. For numerical integration of the full CC equations, the straightforward techniques such as the pointwise Runge-Kutta-Gill have been

superceded by others. Very promising aomng these is Gordon's (24) new piecewise integration in large steps, using a two-function basis expansion in each interval. There is also the invariant imbedding (25) transformation of the CC equations through the integral equation form (with the scattering boundary conditions thus built in) to an alternative set of coupled d.e.'s for the S-matrix elements directly--to be integrated numerically (however, they are nonlinear). A recent Fredholm technique(26) solves the integral equation for the S-matrix directly in a basis expansion extended to the translational coordinate --its chief advantage lies in the ability to treat exchange potentials and other ordinarily paralyzing complications. Another direct integral equation solution has been given by Sams and Kouri (27). Most recently there has been a similar direct solution for the scattering matrix, based upon a parametric reduction (28) of the scattering and potential matrices.

24. R. G. Gordon, J. Chem. Phys. 51,14(1969).

25. D. Secrest and B. R. Johnson, ibid. 45,4556(1966); M. E. Riley and A. Kuppermann, Chem. Phys. Lett. 1,537 (1968).

26. W. P. Reinhardt and A. Szabo, to be publ.

27. W. N. Same and D. J. Kouri, J. Chem. Phys. 51,4809 (1969).

28. H. A. Rabitz, ibid. 55,407(1971).

29. E. Gerjuoy, Ann. Phys. 5,58(1958); see also T.-Y. Wu and T. Ohmura, Quantum Theory of Scattering (Prentice-Hall, Englewood Cliffs, N. J., 1962), §M; the essentially final formal solution was given by L. D. Faddeev, Soviet Phys.-JETP 12,1014(1961).

30. G. Wolken, M. Karplus, and R. G. Gordon, to be publ.

31. D. R. Herschbach, Adv. Chem. Phys. 10,319(1966); with J. H. Birely, J. Chem. Phys. 44,1690(1966); R. E. Minturn, S. Datz, and R. L. Becker, ibid. 44,1149 (1966).

32. K. Takayanagi, Prog. Theor. Phys. 25,S1(1963); J. D. Kelley, 159th Natl. Meeting, Amer. Chem. Soc., L. A., Calif. (1971).

Reprinted from THE JOURNAL OF CHEMICAL PHYSICS, Vol. 52, No. 9, 4807–4817, 1 May 1970
Printed in U. S. A.

Calculation of Transition Probabilities for Collinear Atom–Diatom and Diatom–Diatom Collisions with Lennard-Jones Interaction

VINCENT P. GUTSCHICK* AND VINCENT MCKOY
Arthur Amos Noyes Laboratory of Chemical Physics, California Institute of Technology,† Pasadena, California 91109
AND
DENNIS J. DIESTLER
Department of Chemistry, University of Missouri,‡ St. Louis, Missouri 63121
(Received 10 March 1969)

Numerical integration of the close coupled scattering equations is performed to obtain vibrational transition probabilities for three models of the electronically adiabatic H_2–H_2 collision. All three models use a Lennard-Jones interaction potential between the nearest atoms in the collision partners. The results are analyzed for some insight into the vibrational excitation process, including the effects of anharmonicities in the molecular vibration and of the internal structure (or lack of it) in one of the molecules. Conclusions are drawn on the value of similar model calculations. Among them is the conclusion that the replacement of earlier and simpler models of the interaction potential by the Lennard-Jones potential adds very little realism for all the complication it introduces.

INTRODUCTION

There is current interest in quantum-mechanical treatments of molecular collisions involving excitation of internal degrees of freedom and possibly reaction. The collision systems pose a multichannel scattering problem, commonly solved by the coupled channels (CC) method. The CC equations are coupled differen-

tial equations derived as follows for a nonreactive system: consider a system composed of two asymptotically isolated parts described by internal coordinates $\mathbf{r}_1$, $\mathbf{r}_2$. Let the relative coordinate be given by R. Into the Schrödinger equation,

$$[T(\mathrm{R})+H^0(\mathbf{r}_1,\mathbf{r}_2)+V_I(\mathbf{r}_1,\mathbf{r}_2,\mathrm{R})-E]\psi(\mathbf{r}_1,\mathbf{r}_2,\mathrm{R})=0 \quad (1)$$

(where T is the operator for kinetic energy of relative motion), substitute the state or channel expansion

$$\psi(\mathbf{r}_1,\mathbf{r}_2,\mathrm{R})=\sum_n f_n(\mathrm{R})\phi_n(\mathbf{r}_1,\mathbf{r}_2), \quad (2)$$

where $\{\phi_n\}$ is a complete orthonormal set of the eigenfunctions of H_0,

$$H^0\phi_n=\epsilon_n\phi_n. \quad (3)$$

Left multiplication of Eq. (1) by ϕ_m^* and integration over the coordinates $\mathbf{r}_1$, $\mathbf{r}_2$ yields the CC equations

$$(-T(\mathrm{R})+E-\epsilon_m)f_m(\mathrm{R})=\sum_n V_{mn}(\mathrm{R})f_n(\mathrm{R}), \quad (4)$$

where

$$V_{mn}(\mathrm{R})=\langle\phi_m(\mathbf{r}_1,\mathbf{r}_2)\mid V_I(\mathbf{r}_1,\mathbf{r}_2,\mathrm{R})\mid\phi_n(\mathbf{r}_1,\mathbf{r}_2)\rangle. \quad (5)$$

These equations are solved subject to boundary conditions, generally that asymptotically ($\mid\mathrm{R}\mid\rightarrow\infty$) the relative motion becomes free, i.e.,

$$f_n(\mathrm{R})\sim\exp(i\mathbf{k}_n\cdot\mathrm{R})+\text{scattered waves}. \quad (6)$$

The form of the scattered waves depends upon the dimensionality of the system. The ratio of scattered to incident flux, with flux defined by

$$\mathbf{j}_n(\mathrm{R})=(\hbar/2m)\,\mathrm{Im}(f_n^*\nabla f_n), \quad (7)$$

is the transition probability (one dimension) or cross section (two or three dimensions). As closed-form analytical solutions of Eqs. (4) are not ordinarily obtainable, several techniques have been developed for their accurate numerical integration.[1-5] We developed our own technique of integration using Dirichlet boundary conditions and simple one-step Euler integration. This was the fastest technique available to us at the time of our calculations, though it is now superseded by the reference solution methods of Refs. 4 and 5. The parameters controlling the accuracy of the integration—step size, end points of the integration in the coordinate R, the number of channels included in the expansion Eq. (2), and the accuracy of the numerical integration for the potential matrix elements $V_{mn}(\mathrm{R})$ in Eq. (4)—were chosen such that each individual transition probability was converged to within 1% of its "true" value and detailed balance error, as measured by the quantity

$$e_{mn}=[(P_{mn}-P_{nm})/P_{mn}]\times 100\%, \quad (8)$$

was limited to 0.1%–0.4%, allowing us to report only one probability of each equivalent pair P_{mn}, P_{nm}.

In the first section of this paper, we define the coordinates for the one-dimensional or collinear atom–diatom and diatom–diatom collisions with vibrational excitation. We then specify numerical values of parameters used to define the three models of the H_2–H_2 collision. Two of these models are atom–diatom type, one of which takes the potential for the diatom vibration as the harmonic potential, the other as the Morse potential. The third model is the diatom–diatom type, with each diatom being a harmonic vibrator. Masses of the atoms and diatoms are chosen such that all three models are appropriate for the H_2–H_2 collision—this requires the atom mass to equal the total mass of the diatom. Finally, a Lennard-Jones interaction potential is assumed to operate between the nearest atoms in the collision partners. This is a more realistic choice than the more common one of an exponential potential, at least at low collision energies. In Sec. II we present the numerical results for the transition probabilities. We contrast the physical behavior of the models for qualitative insight into the effects of vibrational anharmonicity and internal structure in the collision partners, and comment briefly on related semiclassical and classical calculations. Finally, we conclude that the simpler exponential interaction potential is preferable to the Lennard-Jones potential because it reproduces transition probabilities for the latter very accurately while requiring far less computing time.

I. NATURE OF THE THREE MODEL CALCULATIONS

A. The Atom–Diatom Collision in One Dimension

The original coordinates for this system are simply the positions x_1, x_2, x_3 of the three masses m_1, m_2, m_3, with m_1-m_2 comprising the bound or diatomic system. The operator for the Hamiltonian minus the energy eigenvalue is

$$H-E=-\frac{\hbar^2}{2m_1}\frac{\partial^2}{\partial x_1^2}-\frac{\hbar^2}{2m^2}\frac{\partial^2}{\partial x_2^2}-\frac{\hbar^2}{2m_3}\frac{\partial^2}{\partial x_3^2}+V_{12}'(x_2-x_1)+V_I'(x_3-x_2)-E. \quad (9)$$

The interaction potential $V_I'(x_1-x_3)$ has been neglected. We show in the Appendix that several consecutive transformations of coordinates can be performed which (1) put the system into the form of an "atom" colliding with another, oscillating atom bound to an equilibrium position—a two-body problem; see Fig. 1—and (2) reduce all coordinates, masses, and potential parameters to a smaller number of dimensionless quantities. The operator $H-E$ in new units and coordinates is

$$H-E=-1/2\mu(\partial^2/\partial x^2)-\tfrac{1}{2}(\partial^2/\partial y^2)+V_{12}(y)+V_I(x-y)-E, \quad (10)$$

where the energy E is exclusive of center-of-mass mo-

tion and is measured in units of $\hbar\omega$, twice the ground-state vibrational energy of the oscillator m_1-m_2. The set of parameters for the collision reduces to E, μ, and the parameters of the two potentials.

Next we make the channel expansion, Eq. (2). The function $\phi_n(y)$ representing bound states of the oscillator are solutions of the eigenvalue equation

$$[-\tfrac{1}{2}(\partial^2/\partial y^2)+V_{12}(y)-\epsilon_n]\phi_n(y)=0. \quad (11)$$

Again, the energies ϵ_n are measured in units of twice the ground-state oscillator energy, so that for the ground state, $\epsilon_1=\frac{1}{2}$. Two models for the oscillator have been used in our calculations: (1) the harmonic oscillator, for which

$$V_{12}(y)=\tfrac{1}{2}y^2,$$
$$\epsilon_n=n-\tfrac{1}{2}, \qquad n=1, 2, 3, \cdots,$$
$$\phi_n(y)=[2^{n-1}(n-1)!]^{-1/2}H_{n-1}(y)\exp(-y^2/2), \quad (12)$$

where H_n is the Hermite polynomial, and (2) the Morse oscillator, for which

$$V_{12}(y)=D_e(e^{-2\beta y}-e^{-\beta y}),$$
$$\epsilon_n=[2(2D_e)^{1/2}/\beta](n-\tfrac{1}{2})-\tfrac{1}{2}\beta^2(n-\tfrac{1}{2})^2,$$
$$\phi_n(y)=N_n\exp(-de^{-\beta y})(2de^{-\beta y})^{(k-2n+1)/2} \times L_{k-n}^{k-2n+1}(2de^{-\beta y}), \quad (13)$$

with

$$d=(2D_e)^{1/2}/\beta,$$
$$k=2d,$$
$$N_n=\text{normalization constant}, \quad (13')$$

and where $L_{a+n}^{n}(x)$ is a generalized Laguerre polynomial. The quantity D_e is the depth of the potential well, and β is an anharmonicity parameter. The Morse oscillator has a finite number of bound states, up to $n_{\max}=k$. The CC equations for both models have the form

$$(d^2/dx^2+k_n^2)f_n(x)=2\mu\sum_{m=1}^{n_{\text{tot}}}V_{nm}(x)f_m(x), \quad (14)$$

with

$$k_n^2=2\mu(E-\epsilon_n),$$
$$V_{nm}(x)=\langle\phi_n(y)\mid V_I(x-y)\mid\phi_m(y)\rangle$$
$$=\int_{-\infty}^{\infty}dy\phi_n(y)V_I(x-y)\phi_m(y),$$

$n_{\text{tot}}=$ number of states retained in the channel expansion. (14')

Our choice of the interaction potential $V_I(x-y)$ is the Lennard-Jones potential with its singularity at $x-y=0$ replaced by a finite step.

$$V_I(x-y)=4\epsilon\{[\sigma/(x-y)]^{12}-[\sigma/(x-y)]^6\}, \quad x-y\geq b$$
$$=V_I(b), \quad x-y<b, \quad (15)$$

although another choice, the exponential potential,

$$V_I(x-y)=C\exp[-\alpha(x-y)] \quad (16)$$

was used to check our method by duplicating some calculations of Secrest and Johnson.[3]

As a shorthand notation for the two models let us use HOLJ for the harmonic oscillator hit by an atom interacting with it by a Lennard-Jones potential, and MOLJ for the Morse oscillator and the same Lennard-Jones interaction (and HOEXP for the harmonic oscillator and the exponential potential). In all of these calculations, the parameters μ, ϵ, σ (and also D_e, β for the MOLJ case) were chosen to represent the collision of two hydrogen molecules, one of which has its vibrational degree of freedom frozen out. The dimensionless values of the parameters are then

$$\mu=0.5,$$
$$\epsilon=5.707\times10^{-3},$$
$$\sigma=46.71,$$
$$D_e=8.3255,$$
$$\beta=0.24886, \quad (17)$$

as converted from dimensioned quantities quoted in Bhatia[6a] and Herzberg[6b] and Herzfeld and Litovitz.[6c] A slight adjustment of β from a calculated value of 0.24840 was made to obtain the proper value of $\epsilon_1=0.5$ for the ground vibrational level. The values of D_e and β allow 16 bound levels for the Morse oscillator.

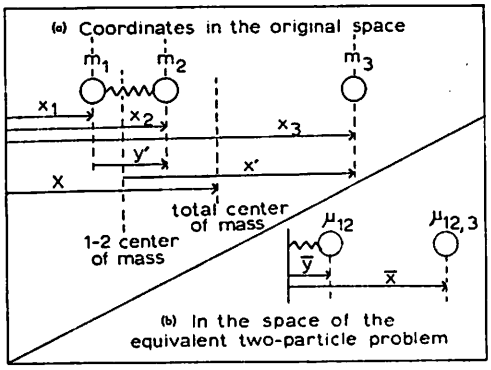

FIG. 1. The original (a) and transformed (b) coordinates for the atom-diatom collision in one dimension.

B. The Diatom-Diatom Collision in One Dimension

The original coordinates for this system are the positions x_i ($i=1, 2, 3, 4$) of the four masses m_i, with m_1-m_2 and m_3-m_4 forming the two bound diatomic systems. Assuming the dominant nonbound interaction

TABLE I. Selection of channels to include in diatom-diatom problem. Maximum excitation of each diatom is to second vibrational level $n_i=2$.[a]

Method (1)—form all possible product states (n_1, n_2) with n_1, n_2 independently ranging from 1 to 4				Method (2)—add the restriction $n_1+n_2\leq 4$	
Channel no.[b]	(n_1, n_2)	Channel no.	(n_1, n_2)	Channel no.[b]	(n_1, n_2)
1	1, 1	9	3, 1	1	1, 1
2	1, 2	10	3, 2	2	1, 2
3	1, 3	11	3, 3	3	2, 1
4	1, 4	12	3, 4	4	1, 3
5	2, 1	13	4, 1	5	2, 2
6	2, 2	14	4, 2	6	3, 1
7	2, 3	15	4, 3	7	1, 4
8	2, 4	16	4, 4	8	2, 3
				9	3, 2
				10	4, 1

[a] Values of n_i to 4 should be included on the basis of atom-diatom model results.
[b] In each selection scheme the open channels are in bold face.

V_I to be between particles 2 and 3, one has

$$H-E=\sum_{i=1}^{4}-(\hbar^2/2m_i)(\partial^2/\partial x_i^2)+V_{12}'(x_1-x_2)+V_{34}'(x_3-x_4)+V_I'(x_2-x_3)-E. \quad (18)$$

In the Appendix we show that successive coordinate transformations, analogous to those used to reduce the atom-diatom problem, put the system into the form of a diatom oscillator hitting a bound oscillating "atom." The system parameters are also made dimensionless. The operator $H-E$ in the transformed coordinates is

$$H-E=-(1/2\mu)(\partial^2/\partial x^2)-\tfrac{1}{2}(\partial^2/\partial y_1^2)-\tfrac{1}{2}(\partial^2/\partial y_2^2)+V_{12}(y_1)+V_{34}(y_2)+V_I(x-y_1-y_2)-E \quad (19)$$

for a system of two *identical* diatoms; the general form is given in the Appendix. Again, E is the energy, exclusive of center-of-mass motion, in units of twice the ground vibrational energy of either oscillator. The set of parameters remains E, μ, and the parameters of the potentials, as in Sec. I.A. The diatom-diatom collision can be made physically equivalent to the atom-diatom collision, so that comparisons of analogous transition probabilities will illustrate the effect of an internal degree of freedom in the incident "particle." In addition, "resonant" energy transfer involving interchange of vibrational quanta between the diatoms with no conversion of translational energy exists for the diatom-diatom case.

The channel expansion of Eq. (2) takes the form

$$\psi(x, y_1, y_2)=\sum_n f_n(x)\phi_{n1}(y_1)\phi_{n2}(y_2), \quad (20)$$

where the ϕ_{n1}, ϕ_{n2} are solutions of eigenvalue equations of the form (10). In our calculations, both diatom oscillators are modeled as harmonic oscillators and the interaction potential is the Lennard-Jones potential; this model is denoted by the shorthand HOHOLJ. System parameters exclusive of the energy E are

$$\mu=0.5,$$
$$\epsilon=5.707\times 10^{-3},$$
$$\sigma=46.71. \quad (21)$$

Test calculations on a model with the exponential potential successfully duplicated the results of Riley.[1]

The CC equations have the general form

$$(\partial^2/\partial x^2+k_n^2)f_n(x)=2\mu\sum_m V_{nm}(x)f_m(x), \quad (22)$$

where

$$k_n^2=2\mu(E-\epsilon_{n1}-\epsilon_{n2}),$$
$$V_{nm}(x)=\langle\phi_{n1}(y_1)\phi_{n2}(y_2)\,|\,V_I(x-y_1-y_2\,|\,\phi_{m1}(y_1)\phi_{m2}(y_2)\rangle.$$

The ordering of states in the expansion (20) becomes significant when we truncate the expansion. Two ways to order or include channels suggest themselves: (1) retain a certain number of states for each oscillator, yielding the correspondence between n and $(n1, n2)$ given in the left-hand columns of Table I, or (2) retain product states $(n1, n2)$ up to a certain energy level $\epsilon_{n1}+\epsilon_{n2}$, yielding the correspondence of n and $(n1, n2)$ given in the right-hand columns of Table I. The second approach places all open channels together at the beginning of the numbering scheme, and makes for a smaller set of coupled equations for similar accuracy; that is, the states $(n1, n2)$ where both $n1$ and $n2$ are high virtual states will be relatively unimportant. The second approach will be used in our HOHOLJ calculations.

Note the occurrence of equivalent channels $(n1, n2)\leftrightarrow(n2, n1)$. These channels are physically distinct; a transition from one to the other involves no conversion of translational into vibrational energy—it is a *resonant* energy transfer.

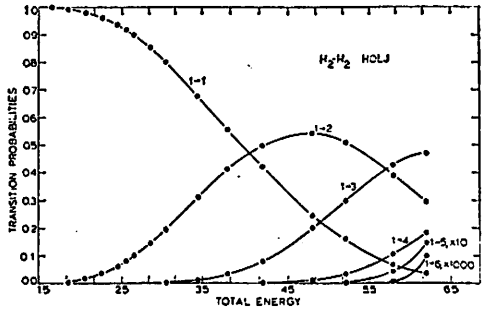

FIG. 2. Energy dependence of the transition probabilities $P(1\to n)$ from the ground state in the atom-diatom problem, HOLJ model.

TABLE II. Calculated transition probabilities for HOLJ model. Numbers in parentheses are negative powers of 10 multiplying result.[a]

	E[b]				
$P_{n\to m}$	1.55	1.65	1.85	2.05	2.25
1→1	0.9999	0.9992	0.9946	0.9835	0.964
1→2	0.121(3)	0.792(3)	0.538(2)	0.165(1)	0.357(1)
2→2	0.9999	0.9992	0.9946	0.9835	0.964

	E					
$P_{n\to m}$	2.45	2.55	2.65	2.85	3.05	3.45
1→1	0.936	0.918	0.898	0.852	0.799	0.674
1→2	0.638(1)	0.815(1)	0.101	0.147	0.199	0.314
1→3		0.506(5)	0.411(4)	0.406(3)	0.170(2)	0.109(1)
2→2	0.936	0.918	0.897	0.843	0.771	0.580
2→3		0.235(3)	0.152(2)	0.100(1)	0.296(1)	0.105
3→3		0.99976	0.9984	0.990	0.969	0.884

	E					
$P_{n\to m}$	3.80	4.20	4.80	5.20	5.80	6.20
1→1	0.555	0.420	0.245	0.157	0.687(1)	0.351(1)
1→2	0.412	0.498	0.543	0.510	0.394	0.296
1→3	0.323(1)	0.799(1)	0.201	0.300	0.427	0.470
1→4	0.421(4)	0.855(3)	0.106(1)	0.322(1)	0.105	0.183
1→5			0.107(4)	0.264(3)	0.422(2)	0.149(1)
1→6					0.350(5)	0.100(3)
2→2	0.384	0.179	0.104(1)	0.222(1)	0.175	0.299
2→3	0.202	0.313	0.383	0.328	0.148	0.416(1)
2→4	0.640(3)	0.870(2)	0.631(1)	0.136	0.258	0.297
2→5			0.123(3)	0.228(2)	0.241(1)	0.644(1)
2→6					0.341(4)	0.773(3)
3→3	0.755	0.536	0.177	0.313(1)	0.387(1)	0.134
3→4	0.982(2)	0.698(1)	0.238	0.326	0.297	0.180
3→5			0.108(2)	0.137(1)	0.878(1)	0.170
3→6					0.233(3)	0.401(2)
4→4	0.989	0.921	0.676	0.421	0.805(1)	0.364(2)
4→5			0.124(1)	0.834(1)	0.256	0.317
4→6					0.156(2)	0.186(1)
5→5			0.986	0.900	0.612	0.338
5→6					0.146(1)	0.945(1)
6→6					0.9835	0.882

[a] Calculated values of P_{nm} and P_{mn} were always well within 1% of each other. To avoid redundancy, only the former are given.

[b] Energy units are $\hbar\omega$, twice the ground-state vibrational energy of the diatom.

II. RESULTS OF MODEL CALCULATIONS

Tables II–IV present our calculated transition probabilities for the HOLJ, MOLJ, and HOHOLJ models. The total error in these results is in the range of 1% or less. The behavior of selected probabilities P_{mn} as functions of energy is illustrated in Figs. 2-6. The clearest feature for both atom–diatom models HOLJ and MOLJ, which cover significant energy ranges, is the oscillation of the P_{mn}. For instance, the elastic transition probability P_{22} in the HOLJ model decreases steadily until it reaches a deep minimum near $E=4.9$; then, despite the opening of an additional *in*elastic channel at $E=4.5$, P_{22} begins to rise rapidly. This is "caused" by the

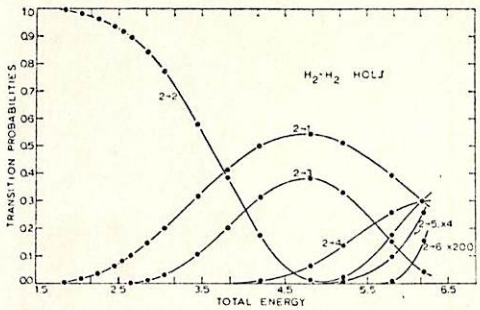

FIG. 3. Energy dependence of the transition probabilities $P(2\rightarrow n)$ from the first excited state in the atom–diatom problem, HOLJ model.

downward turns in probabilities P_{21} and P_{23}. We see a similar behavior in transitions from initial states 1 and 3, P_{1n} and P_{3n}. Comparing transitions according to their initial state, we note that the coupled oscillations in probabilities set in at a lower value of initial kinetic energy $E-\epsilon_n$, the higher the initial state n.

This oscillatory behavior has been found in similar atom–diatom model systems by previous workers. Shuler and Zwanzig[7] found sharp-peaked oscillations for all transitions in their exact but specialized quantum-mechanical treatment of the harmonic diatom and the hard-sphere interaction potential,

$$V_I(x-y)=0, \qquad x-y>0.$$
$$\infty, \qquad x-y=0. \tag{23}$$

The exact result of Secrest and Johnson[3] for several HOEXP models show maxima in inelastic probabilities. The exact semiclassical results of Rapp and Sharp[8] for a HOEXP-like model show regular oscillations. The oscillations in our results and the results quoted above are real, although there have been many approximate calculations in which the use of low-order perturbation theory or the artificial exclusion of most of the channels in expansion (2) has led to a spurious effect.

A major part of the analysis of our results is the

TABLE III. Calculated transition probabilities for MOLJ model.[a]

	E[b]			
$P_{n\rightarrow m}$	1.55	1.90	2.30	2.75
1→1	0.99983	0.9958	0.980	0.939
1→2	0.165(3)	0.417(2)	0.198(1)	0.604(1)
1→3				0.129(3)
2→2	0.99983	0.9958	0.980	0.931
2→3				0.819(2)
3→3				0.9917
	E			
$P_{n\rightarrow m}$	3.40	4.15	4.45	4.85
1→1	0.854	0.724	0.662	0.582
1→2	0.142	0.255	0.302	0.354
1→3	0.314(2)	0.204(1)	0.345(1)	0.602(1)
1→4	0.159(5)	0.306(3)	0.977(3)	0.320(2)
1→5		0.138(6)	0.317(5)	0.394(4)
1→6				0.198(7)
2→2	0.780	0.508	0.391	0.249
2→3	0.779(1)	0.229	0.287	0.347
2→4	0.868(4)	0.809(2)	0.198(1)	0.475(1)
2→5		0.623(5)	0.111(3)	0.104(2)
2→6				0.764(6)
3→3	0.915	0.643	0.493	0.296
3→4	0.412(2)	0.108	0.182	0.281
3→5		0.182(3)	0.230(2)	0.145(1)
3→6				0.180(4)
4→4	0.9958	0.878	0.756	0.531
4→5		0.598(2)	0.407(1)	0.137
4→6				0.371(3)
5→5		0.9938	0.957	0.838
5→6				0.919(2)
6→6				0.9904

[a] Calculated values of P_{nm} and P_{mn} were always well within 1% of each other. To avoid redundancy, only the former are given.

[b] Energy units are $\hbar\omega$, twice the ground-state vibrational energy of the diatom.

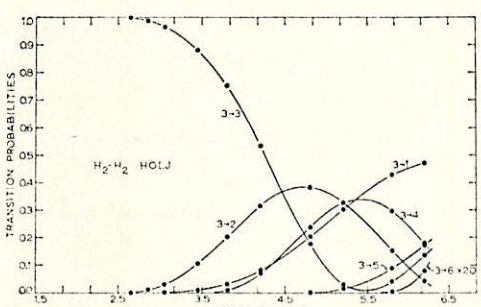

FIG. 4. Energy dependence of the transition probabilities $P(3\rightarrow n)$ from the second excited state in the atom–diatom problem, HOLJ model.

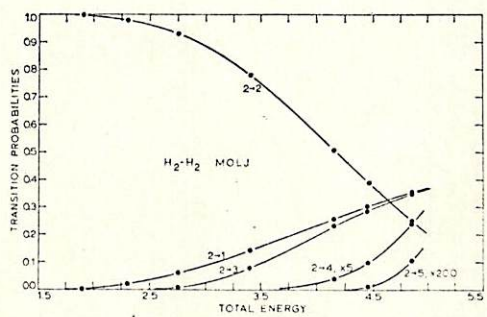

FIG. 5. Energy dependence of the transition probabilities $P(2\rightarrow n)$ from the first excited state in the atom–diatom problem, MOLJ model.

TABLE IV. Calculated transition probabilities for HOHOLJ model.[a]

	E[b]					
$P_{n\to m}$	2.05	2.15	2.35	2.55	2.75	2.95
11→11[c]	0.99990	0.99934	0.9956	0.987	0.972	0.951
11→12	0.508(4)	0.329(3)	0.219(2)	0.656(2)	0.140(1)	0.245(1)
12→12	0.9929	0.980	0.950	0.914	0.872	0.825
12→21	0.707(2)	0.194(1)	0.474(1)	0.789(1)	0.114	0.150
	E					
$P_{n\to m}$	3.08	3.15	3.35	3.55		
11→11	0.934	0.923	0.890	0.853		
11→12	0.328(1)	0.382(1)	0.547(1)	0.731(1)		
11→13	0.183(5)	0.680(5)	0.648(4)	0.261(3)		
11→22	0.366(5)	0.136(4)	0.130(3)	0.523(3)		
12→12	0.792	0.773	0.714	0.650		
12→21	0.175	0.188	0.224	0.258		
12→13	0.192(3)	0.603(3)	0.381(2)	0.108(1)		
12→22	0.104(3)	0.329(3)	0.214(2)	0.627(2)		
12→31	0.143(4)	0.548(4)	0.524(3)	0.204(2)		
13→13	0.980	0.963	0.909	0.846		
13→22	0.200(1)	0.360(1)	0.848(1)	0.136		
13→31	0.110(3)	0.352(3)	0.203(2)	0.556(2)		
22→22	0.960	0.927	0.826	0.715		

[a] Calculated values of $P(n1, n2)\to(n1', n2')$ that should be equal among themselves by time-reversal invariance or symmetry were negligibly different. Only one member is given to avoid redundancy.

[b] Energy units are $\hbar\omega_{12}=\hbar\omega_{34}=\hbar\omega$, twice the ground-state vibrational energy of either diatom.

[c] The transition $(n1, n2)\to(n1', n2')$ is abbreviated to $n1n2\to n1'n2'$.

comparison and contrast of the three models for the H_2–H_2 collision. Suitable quantities for comparison include analogous transition probabilities (as 1→2 HOLJ, 1→2 MOLJ, 11→12⊕11→21 HOHOLJ), net energy transfer from analogous initial states, and relative strengths of multiquantum jumps. Contrasts of HOLJ and MOLJ models will tell us something about the effects of anharmonicity, and contrasts of HOLJ and HOHOLJ will help reveal the effect of internal structure in the incident particle. At the same time, examinations of models individually show the basic energy behavior of the probabilities and other properties that are as instructive as the obvious contrasts between models. Specific items we can study, both within and between models, include comparisons of (1) all transi-

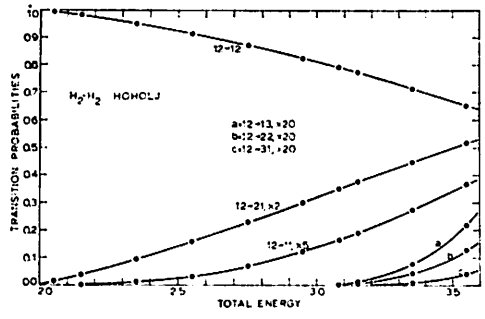

FIG. 6. Energy dependence of the transition probabilities $P(12\to mn)$ in the diatom-diatom problem, HOHOLJ model. The initial state 1–2 has one of the diatoms in its ground state, the other in its first excited state.

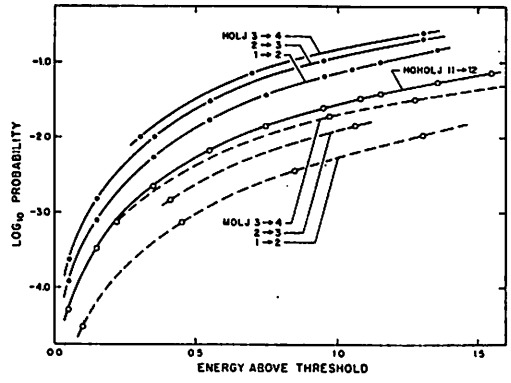

FIG. 7. Demonstration of very similar energy dependence for one-quantum jumps in all three models of the H_2–H_2 collision, HOLJ, MOLJ, HOHOLJ. The curves of $\log_{10}$(probability) have been biased by −0.75 in the MOLJ cases for clarity.

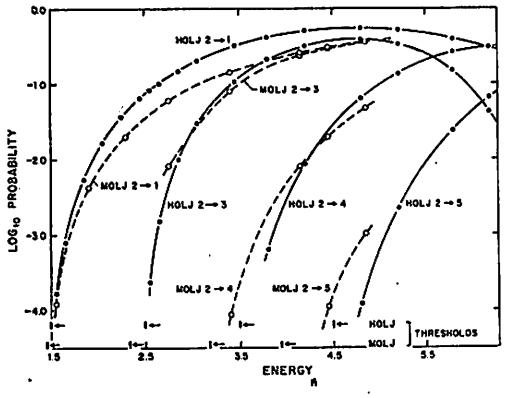

FIG. 8. Comparison of all transition probabilities $P(2\to n)$ from the first excited state. The two atom–diatom models HOLJ and MOLJ are both represented.

tions of a given type, such as one-quantum jumps $P_{n,n+1}$, for various initial states n, (2) all transitions P_{nm} from a given initial state n, (3) net energy transfer (translational to vibrational) from each state n, defined for the atom–diatom models as

$$\langle \Delta E_n \rangle = \sum_m{}' P_{nm}(\epsilon_m - \epsilon_n), \tag{24}$$

where the ϵ_i are the energy eigenvalues for the diatom vibration. The diatom–diatom model has several types of energy transfer that will be defined later.

Figure 7 presents a logarithmic plot of several one-quantum jump probabilities for each of the three models. The abscissa in each case is energy above threshold $E_{ex}=E-\epsilon_{n+1}$, rather than initial kinetic energy. The striking fact brought out by the logarithmic plot is that all the $P_{n,n+1}$ for a given model behave much like

$$P_{n,n+1}(E) = \mathrm{Const}_n\, f(E_{ex}), \tag{25}$$

with $f(_{ex})$ the same for all n. Further, $f(E)$ is very similar for the HOLJ and HOHOLJ models, while $\log f(E)$ for MOLJ has a smaller slope at the lowest energies. Pursuing this point of similarity, we turn to the actual magnitudes of probabilities at low energy. For the analogous transitions 11→12⊕11→21 HOHOLJ and 1→2 HOLJ, we find

$$(P_{11\to 12}+P_{11\to 21})_{\mathrm{HOHOLJ}}/(P_{12})_{\mathrm{HOLJ}} \approx 0.8 \tag{26}$$

at low energy. Not only do these transitions have similar $f(E)$ or "slopes," but their magnitudes are close, being reduced for the HOHOLJ case by the extra adiabaticity or softness introduced into the collision process by the extra internal degree of freedom. That the change from HOLJ to HOHOLJ is principally the addition of a very modest amount of adiabaticity is supported by comparing the 11→12 and 21→22 HOHOLJ probabilities. The two values are extremely close at low energies, indicating again that the initial state of our extra internal degree of freedom has little effect of itself on transition probabilities—which would not be true if the extra degree of freedom coupled strongly to translation. However, it does couple strongly to the vibration of the other diatom, giving rise to highly favored resonant energy transfers of the type 12→21. The latter transitions may be of independent interest, but they do not drain much probability from other transitions at modest energies.

Proceeding to the HOLJ–MOLJ comparison, we find the ratio $(P_{12})_{\mathrm{MOLJ}}/(P_{12})_{\mathrm{HOLJ}}$ is quite small—around 0.3–0.4. This is readily explained by the lower coupling between adjacent states of the anharmonic oscillator (compared to that for a harmonic oscillator) induced by a potential that is essentially linear in the oscillator coordinate. This near linearity in the coordinate y holds near the classical turning point x_t, where $V_I(x_t-\langle y\rangle)=E-\epsilon_n$, for our Lennard-Jones potential—and it is the region of x_t that is most important. The problem of why MOLJ one-quantum jumps have a different "slope" at low energies than HOLJ jumps cannot be commented on with our calculations limited to so few energies.

Figure 8 presents a comparison of the second type, among all transitions from initial state 2 (P_{21}, P_{23}, P_{24}, P_{25}) for both atom–diatom models. It is also a logarithmic plot, and the abcissa is appropriately the total energy E. A clear feature is that the horizontal or energy gaps between adjacent curves $2\to n$, $2\to n+1$ are widening as n increases. That is, in either of the two models, the higher the quantum jump, the more slowly the probability grows. The explanation is again in the essential linearity of the interaction potential at the classical turning point; the first-order coupling of a final state to the initial state is a very strongly decreasing function of the number of quantum jumps in the transition. This argument does not hold as well for the anharmonic MOLJ model, and so the energy intervals between the various curves do not widen as

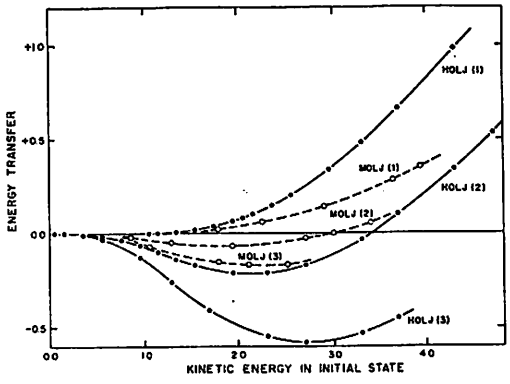

FIG. 9. Atom–diatom collision: net transfer of energy from translation to diatom vibration as a function of the initial state (n) and of the kinetic energy in the initial state. Both HOLJ and MOLJ models are represented.

rapidly here, even after we discount the decreasing intervals between thresholds.

We have no HOHOLJ results for transitions higher than two-quantum jumps, and these only from the ground state. Yet the HOHOLJ model has a greater variety of transition types or processes than the atom–diatom models. Finding the relative magnitudes of the different processes is a worthwhile task. The processes we distinguish, and examples of each, are:

E—Elastic: 11→11, 12→12

R—Resonant: no net quantum jump in the pair of diatoms, i.e., opposite jumps in each diatom: 12→21, 22→13

SR—Semiresonant: opposite jumps of different order in each diatom: 12→31

NR—Nonresonant:

(a) One-quantum jump: 11→12, 22→12

(b) Two-quantum jump: 11→13

(c) Double one-quantum jump: 11→22

The HOHOLJ results at the modest energy $E=3.55$ show that the strengths of processes generally follow the order

$$\mathrm{E}>\mathrm{R}>\mathrm{NR(a)}>\mathrm{SR}>\cdots, \tag{27}$$

reflecting the weakness of translational–vibrational coupling compared to vibrational–vibrational (V–V) coupling. There are V–V processes that are weak, as the 13→31 transition involving concerted two-quantum jumps that are approximately forbidden in first order.

Our final study is of energy transfer. Figure 9 plots $\langle\Delta E_n\rangle$ for both atom–diatom models from initial states 1, 2, and 3 as functions of initial kinetic energy. MOLJ has about 40% the energy transfer efficiency of HOLJ, from the initial states 1 or 2. The energy transfer in state 2 reaches a node at lower energy for MOLJ than HOLJ, reflecting the earlier opening up of new channels for MOLJ. The disparity in form for HOLJ and MOLJ energy transfer appears to be very pronounced for high initial states.

To define the measure of energy transfer for diatom–diatom collisions, we must denote the subsystems or degrees of freedom between which the transfer occurs. These subsystems are translation or "tr," diatom 1–2 or "d" (playing the same role as the diatom in atom–diatom collisions), and diatom 3–4 or "a" (playing the same role as the atom). The energy transfers most directly comparable to the atom–diatom results are tr→a+d≡tr→all, tr→d (not equal in general to tr→a; "d" and "a" may be initially in different states, making for distinguishability in this otherwise symmetric system), and tr+a→d≡all→d. Figure 10 presents these three $\langle\Delta E\rangle$ functions for HOHOLJ in initial states 11, 12, and 13, plotted as functions of initial kinetic energy. ΔE(tr→d) is very nearly identical for states 11 and 12 for comparable distances above their respective thresholds, corresponding to our finding that the state of a does not much affect the coupling of d to tr. There is

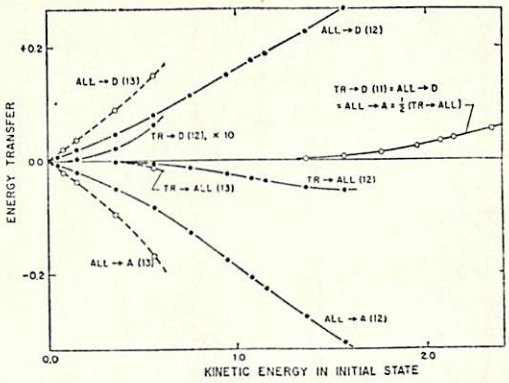

FIG. 10. Diatom–diatom collision, HOHOLJ model: net transfer of energy between the various degrees of freedom (e.g., TR = translation; see text for symbol meaning), as a function of initial state (n_1n_2) and of the kinetic energy in the initial state.

also the expected trend, that ΔE(all→d) increases strongly as the state of "a" is raised. As there is nothing surprising within Fig. 10, we proceed to compare HOHOLJ with HOLJ via their ratio $\Delta E(\mathrm{tr}\rightarrow\mathrm{all})/\Delta E$ for analogous initial states. For HOHOLJ state 11 and HOLJ state 1, the ratio is around 0.8, reflecting the extra adiabaticity of the diatom–diatom case. For HOHOLJ state 21 and HOLJ state 2, the ratio is about 0.4, probably due to the drain of the resonant process 12→21. The same ratio occurs in the comparison HOHOLJ 31↔HOLJ 3 and in the weaker comparison HOHOLJ 22↔HOLJ 3.

We may draw a number of conclusions from our results, particularly regarding the value of similar model calculations on intermolecular energy transfer. Despite the limitations of our models—one-dimensionality, a restricted and modeled interaction potential, and the simplicity of the models of the diatoms—we have extracted a number of physical insights into the collision of two fairly stiff diatoms, if not into the actual H_2–H_2 collision. The effects of anharmonicity and of internal degrees of freedom, and the relative magnitudes of different processes are among the insights. Certainly, calculations on a wider sampling of collision partners within the same general modeling scheme can be recommended as a practical and valuable project; the computing times are moderate. We are also able to suggest some precautions and some simplifications in modeling a collision system. First, the introduction of all the internal degrees of freedom of the collision partners is not as necessary for reasonably accurate calculations as a fair degree of anharmonicity in the vibrations. Neither complication can really be ignored and semiempirical corrections based on careful studies of additional systems are probably desirable. Secondly, the choice of analytic form for the interaction potential is not nearly as important as the careful estimation of the parameters for the chosen form. To support this claim

we turn to some results of A. Wagner of this laboratory. In entirely similar calculations he employed HOEXP and HOHOEXP models for the H_2–H_2 system with the EXP (exponential) potential parameter α carefully fitted by various least-squares techniques to the Lennard-Jones parameters σ, ϵ. His calculations duplicated ours within several percent for all but the highest quantum jumps at the highest energies, where one probability might be off as much as a factor of 2. Let us consider that neither LJ nor EXP potentials are terribly realistic, and that the change in probabilities in switching from one to the other is less than the change produced by a very minor shift in the parameters of either one. We see no reason to retain the LJ potential with its attendant great increase in complexity and computing time,[9] at least in treating systems such as ours where the energy quanta exchanged in collision are considerably larger than the small attractive well in the LJ potential. If one *must* use a potential that has an appreciable attractive portion, as a chemical "well," or if one must do accurate calculations, his best choice of potential is one tabulated numerically. If one is satisfied with as simple a potential as the exponential, he should choose his parameters very carefully. A much-needed study is the development of simple but more adequate model intermolecular potentials, particularly for three-dimensional systems.

ACKNOWLEDGMENTS

One of us (D. D.) wishes to thank the California Institute of Technology for its hospitality. We would like to thank A. Wagner, N. W. Winter, and D. G. Truhlar of the California Institute of Technology for helpful discussions. We are particularly grateful to Merle E. Riley, presently at the Harvard College Observatory, for a thorough and helpful criticism of the manuscript and for other suggestions.

APPENDIX

Transformation to Dimensionless Coordinates for the Atom–Diatom Problem

Figure 1(a) shows the original coordinate system. The first step is to separate the center of mass motion in Eq. (9), by defining new coordinates

$$X=(m_1x_1+m_2x_2+m_3x_3)/M, \qquad M=m_1+m_2+m_3$$

$$=\text{coordinate of center of mass of entire system.}$$

$$x'=x_3-(m_1x_1+m_2x_2)/m, \qquad m=m_1+m_2$$

$$=\text{distance between particle 3 and center of mass of system 1–2,}$$

$$y'=x_2-x_1, \tag{A1}$$

and corresponding masses

$$M\rightarrow X,$$

$$\mu_{12,3}=mm_3/M\rightarrow x'$$

$$\mu_{12}=m_1m_2/m\rightarrow y'. \tag{A2}$$

The new form of the operator $H-E$ is

$$-\frac{\hbar^2}{2M}\frac{\partial^2}{\partial X^2}-\frac{\hbar^2}{2\mu_{12,3}}\frac{\partial^2}{\partial x'^2}-\frac{\hbar^2}{2\mu_{12}}\frac{\partial^2}{\partial y'^2}$$
$$+V_{12}(y')+V_I[x'-(m_1/m)y']-E. \tag{A3}$$

Now remove the center-of-mass motion; write

$$E=E_{\text{tr}}+E_{\text{vib}}$$
$$=E_{\text{tr}}^{\text{cm}}+E_{\text{tr}}^{\text{rel}}+E_{\text{vib}}, \tag{A4}$$

and remove the operator

$$-(\hbar^2/2m)(\partial^2/\partial X^2)-E_{\text{tr}}^{\text{cm}}=0 \quad \text{(for eigenstates)}. \tag{A5}$$

Next, place x' and y' on an equal footing by defining

$$x'=(m_1/m)(\bar{x}+y_0'), \quad \text{or} \quad \bar{x}=(m/m_1)x'-y_0',$$

$$y'=\bar{y}+y_0', \quad \text{or} \quad \bar{y}=y'-y_0', \tag{A6}$$

where y_0' is the equilibrium value of y'. The corresponding masses are

$$\bar{\mu}=(m_1^2/m^2)\mu_{12,3}=m_1^2m_3/mM\rightarrow\bar{x},$$

$$\mu_{12}\rightarrow\bar{y}, \tag{A7}$$

and the operator $H-E$ becomes

$$-\frac{\hbar^2}{2\bar{\mu}}\frac{\partial^2}{\partial\bar{x}^2}-\frac{\hbar^2}{2\mu_{12}}\frac{\partial^2}{\partial\bar{y}^2}+\bar{V}_{12}(\bar{y})+\bar{V}_I(\bar{x}-\bar{y})-\bar{E}, \tag{A8}$$

where

$$\bar{V}_{12}(\bar{y})=V_{12}(\bar{y}+\bar{y}_0'),$$

$$\bar{V}_I(\bar{x}-\bar{y})=V_I[(m_1/m)(\bar{x}-\bar{y})],$$

$$\bar{E}=E-E_{\text{tr}}^{\text{cm}}. \tag{A9}$$

Lastly, divide the whole of Eq. (A8) by $\hbar\omega=$ twice the ground-state vibrational energy of the 1–2 system, and absorb the factors $\hbar^2/2\mu_i$ into the derivative terms. Define

$$x=(\mu_{12}\omega/\hbar)^{1/2}\bar{x},$$

$$y=(\mu_{12}\omega/\hbar)^{1/2}\bar{y},$$

$$\mu=\bar{\mu}/\mu_{12}=m_1m_3/Mm_2,$$

$$E_r=\bar{E}/\hbar\omega \tag{A10}$$

to obtain Eq. (10)

$$-(1/2\mu)(\partial^2/\partial x^2)-\tfrac{1}{2}(\partial^2/\partial y^2)+V_{12}'(y)+V_I'(x-y)-E_r,$$

where

$$V_{12}'(y)=\frac{\bar{V}_{12}[(\hbar/\mu_{12}\omega)^{1/2}y]}{\hbar\omega}$$

$$=\frac{V_{12}[(\hbar/\mu_{12}\omega)^{1/2}y+y_0']}{\hbar\omega},$$

$$V_I'(x-y)=\frac{\bar{V}_I[(\hbar/\mu_{12}\omega)^{1/2}(x-y)]}{\hbar\omega}$$

$$=\frac{V_I[(m/m_1)(\hbar/\mu_{12}\omega)^{1/2}(x-y)]}{\hbar\omega}. \quad \text{(A11)}$$

The transformations in (A11) will change all parameters of the original potentials into dimensionless quantities, and in some cases reduce the number of parameters in V_{12} by one.

Transformation to Dimensionless Coordinates for the Diatom-Diatom Problem

We separate the center-of-mass motion from Eq. (18) by defining the coordinates and corresponding masses

$$X=\sum^{4} m_i x_i/M, \qquad M=m_1+m_2+m_3+m_4,$$

$$y_{12}'=x_2-x_1, \qquad \mu_{12}=m_1m_2/m_{12} \qquad (m_{ij}=m_i+m_j),$$

$$y_{34}'=x_4-x_3, \qquad \mu_{34}=m_3m_4/m_{34},$$

$$x'=(m_3x_3+m_4x_4)/m_{34}-(m_1x_1+m_2x_2)/m_{12}, \qquad \mu_{12,34}=m_{12}m_{34}/M$$

$$=\text{distance between the centers of mass of systems 1-2 and 3-4.} \quad \text{(A12)}$$

The operator $H-E$, dropping the operator (A5), is

$$-\frac{\hbar^2}{2\mu_{12}}\frac{\partial^2}{\partial y_{12}'^2}-\frac{\hbar^2}{2\mu_{34}}\frac{\partial^2}{\partial y_{34}'^2}-\frac{\hbar^2}{2\mu_{12,34}}\frac{\partial^2}{\partial x'^2}+V_{12}(y_{12}')$$

$$+V_{34}(y_{34}')+V_I\left(x'-\frac{m_1}{m_{12}}y_{12}'-\frac{m_4}{m_{34}}y_{34}'\right)-E. \quad \text{(A13)}$$

Next put x' and y_{12}' on the same footing, by defining new coordinates and masses,

$$\bar{x}=(m_{12}/m_1)x'-y_{12}^0-\bar{\gamma}y_{34}^0, \qquad \bar{\mu}_{12,34}=(m_1^2/m_{12}^2)\mu_{12,34},$$

$$\bar{\gamma}=m_{12}m_4/m_1m_{34},$$

$$\bar{y}_{12}=y_{12}'-y_{12}^0, \qquad \mu_{12},$$

$$\bar{y}_{34}=y_{34}'-y_{34}^0, \qquad \mu_{34}. \quad \text{(A14)}$$

The potential terms in $H-E$ become

$$\bar{V}_{12}(\bar{y}_{12})+\bar{V}_{34}(\bar{y}_{34})+\bar{V}_I(\bar{x}-\bar{y}_{12}-\gamma\bar{y}_{34})=V_{12}(\bar{y}_{12}+y_{12}^0)$$

$$+V_{34}(\bar{y}_{34}+y_{34}^0)+V_I[(m_1/m_{12})(\bar{x}-\bar{y}-\bar{\gamma}\bar{y}_{34})]. \quad \text{(A15)}$$

The operator is finally made dimensionless by dividing by $\hbar\omega_{12}$ and absorbing dimensional factors into the second differential operators. Define

$$x=(\mu_{12}\omega_{12}/\hbar)^{1/2}\bar{x},$$

$$y_{12}=(\mu_{12}\omega_{12}/\hbar)^{1/2}\bar{y}_{12},$$

$$y_{34}=(\mu_{34}\omega_{34}/\hbar)^{1/2}\bar{y}_{34},$$

$$\bar{\mu}=\mu_{12,34}'/\mu_{12}=m_1m_{34}/M'm_2,$$

$$\gamma=(m_2/m_3)(\mu_{34}\omega_{12}/\mu_{12}\omega_{34})^{1/2} \quad \text{(A16)}$$

to obtain the generalization of Eq. (19),

$$H-E=-(1/2\mu)(\partial^2/\partial x^2)-\tfrac{1}{2}(\partial^2/\partial y_{12}^2)$$

$$-(\omega_{34}/\omega_{12})(\partial^2/\partial y_{34}^2)+V_{12}'(y_{12})+V_{34}'(y_{34})$$

$$+V_I'(x-y_{12}-\gamma y_{34}). \quad \text{(A17)}$$

The potentials are related to their original forms by

$$V_{12}'(y_{12})=V_{12}[(\hbar/\mu_{12}\omega_{12})^{1/2}y_{12}+y_{12}^0]/\hbar\omega_{12},$$

$$V_{34}'(y_{34})=V_{34}[(\hbar/\mu_{34}\omega_{34})^{1/2}y_{34}+y_{34}^0]/\hbar\omega_{12},$$

$$V_I'(x-y_{12}-\gamma y_{34})$$

$$=V_I[(m_1/m_{12})(\hbar/\mu_{12}\omega_{12})^{1/2}(x-y_{12}-\gamma y_{34})]/\hbar\omega_{12}. \quad \text{(A18)}$$

* National Science Foundation Predoctoral Fellow, 1966-1969.
† Contribution No. 3909.
‡ Presently at the Department of Chemistry, Purdue University, Lafayette, Ind. 47907.

[1] M. E. Riley, thesis, California Institute of Technology, 1968 (unpublished); M. E. Riley and A. Kuppermann, Chem. Phys. Letters 1, 537 (1968).
[2] S-K Chan, J. C. Light, and J. Lin, J. Chem. Phys. 49, 86 (1968).
[3] D. Secrest and B. R. Johnson, J. Chem. Phys. 45, 4556 (1966). For earlier work in multichannel invariant imbedding consult F. Calogero, *Variable Phase Approach to Potential Scattering* (Academic Press Inc., New York, 1967), Chap. 19.
[4] R. Gordon, J. Chem. Phys. 51, 4 (1969).
[5] A. Cheung and D. Wilson, J. Chem. Phys. 51, 4733 (1969).
[6] (a) A. B. Bhatia, *Ultrasonic Absorption* (Oxford University Press, 1967), for values of ϵ and σ; (b) G. Herzberg, *Spectra of Diatomic Molecules* (D. Van Nostrand, Co., Inc., Princeton, N.J., 1939), for values of D_e and β; (c) K. F. Herzfeld and T. A. Litovitz, *Absorption and Dispersion of Ultrasonic Waves* (Academic Press Inc., New York, 1959).
[7] K. E. Shuler and R. Zwanzig, J. Chem. Phys. 33, 1778 (1960).
[8] D. Rapp and T. E. Sharp, J. Chem. Phys. 38, 2641 (1963).
[9] In HOLJ computations, 90%–95% of the net computing time was spent in calculating the potential matrix elements $V_{mn}(x)$ and only 5%–10% on actual solution of the CC equations. In HOEXP calculations, only about 1%–2% of the time was spent computing potential matrix elements. Similar percentage figures would hold even for the CC integration techniques of Refs. 4 and 5.

Appendix. Our CC Integration Technique

At the time of our calculations, there were essentially two possible numerical integration techniques. First was straightforward numerical integration in the coordinate $\underline{x}$, statring from some $\underline{x_o}$ where $\Psi(\underline{x},\underline{y}) \simeq 0$. A standard integrator such as Runge-Kutta-Gill is used. A number $\underline{n_s}$ of linearly-independent solutions, $\underline{n_s} \geq \underline{n_{op}}$ ($\underline{n_{op}}$ = number of open channels) is required, each of the form

$$\Psi_k = \sum_{n=1}^{n_{tot}} f_n^{(k)}(x)\phi_n(y). \qquad (1)$$

These solutions are begun with the proper physical boundary condition (b.c.) that $\underline{f_n^{(k)}(x_o)} = 0$ but do not obey the proper scattering boundary conditions for pure states in the potential-free region $x \to \infty$. These conditions are that right-incident waves exist in only one channel $\underline{n}$, with scattered waves in all channels:

$$\Psi^I(x,y) = \sum_{n=1}^{n_{tot}} F_n^{(I)}(x)\phi_n(y)$$

$$F_n^{(I)}(x) \underset{x\to\infty}{\to} \delta_{nI}e^{-ik_nx} + A_n{}^I e^{+ik_nx} .$$

Only an integral equation can build in these conditions (and such a technique was developed about the same time by M.E. Riley; see ref. 25 of the introduction). Our $\underline{n_s}$ independent solutions behave asymptotically as

$$f_n^{(k)}(x) \to B_n^k e^{-ik_nx} + A_n^k e^{+ik_nx} . \qquad (2)$$

They must be linearly combined to meet the scattering b.c.,

$$F_n^{(I)}(x) = \sum_{k=1}^{n_s} c_k^{(I)} f_n^{(k)}(x).$$

The n_s straightforward integrations with independent starting b.c., such as

$$\frac{d}{dx} f_n^{(k)}(x) = \delta_{nk} , \qquad (3)$$

must be dressed up to be practical. As the solutions are propagated from x_o to some x_f essentially in the potential-free region, the virtual channels with their exploding components

$$f_n^{(k)} \rightarrow B_n^k e^{+|k_n| x} + A_n^k e^{-|k_n| x}$$

dominate the couplings of all the other $f_n^{(k)}$ and cause practical linear dependence in the solutions. Periodic reorthogonalization, as in the DRILL method developed by M. E. Riley (Ph.D. thesis, Caltech, 1968) is the easiest solution.

The second technique was the recently-developed total finite-difference (FD) method (D. J. Diestler and V. McKoy, J. Chem. Phys. 48,2941(1968)). It is an extension of sorts of the previous method which discretizes one coordinate, x, to effect a numerical solution. FD discretizes both x and y to obtain matrix equations for the wavefunction at the mseh points (x_i, y_i). It does not have linear dependence problems for reasons much the same as in our final method discussed shortly. However, it is very time-consuming for most physical problems with large ranges of x, y to be

covered. It is more useful for small regions of strong coupling and especially for the interaction region of reactive scattering (Diestler and McKoy, ibid. 48,2951(1968)) where we do not wish to commit ourselves to a channel expansion in one or the other arrangement channel. In our type of problem, however, we should make use of our knowledge of the uncoupled $\underline{y}$-motion--i.e., of the $\phi_n(\underline{y})$; we require fewer $\phi_n(\underline{y})$ than mesh points in $\underline{y}$ to cover the $\underline{y}$-space. Thus we converted FD to the CC equations and achieved the fastest method to date, which we called finite-difference-matrix (FDM). Consider how we would solve Eq. (14) of the text numerically: discretize it in $\underline{x}$ as (suppress the index $\underline{k}$ for now)

$$(\frac{1}{h^2}\,\delta_o^2 + k_n^2)f_n(x) = 2\mu\sum_m V_{nm}(x)f_m(x),$$

where the difference operation δ_o^2 is

$$\delta_o^2 f_n(x) = f_n(x+h) - 2f_n(x) + f_n(x-h)$$

and $\underline{h}$ is clearly the mesh spacing in $\underline{x}$. Rewrite this as

$$\left[-\frac{2}{h^2} + k_n^2 - 2\mu V_{nn}(x)\right] f_n(x) + \frac{1}{h^2} f_n(x+h)$$

$$+ \frac{1}{h^2} f_n(x-h) - 2\mu\sum_{m\neq n} V_{nm}(x)f_m(x) = 0. \qquad (4)$$

To get one of the linearly-independent solutions $\{f_n^{(k)}(x)\}$, values of the $f_n^{(k)}(x)$ must be specified at two points $\underline{x_1}$, $\underline{x_2}$. Note that the choice $\underline{x_1} = \underline{x_o}$, $\underline{x_2} = \underline{x_o + h}$ nearly corresponds to the b.c. (3) for the old method of solution. A more appropriate choice of $\underline{x_1}$, $\underline{x_2}$ would be $\underline{x_o}$

and $\underline{x_f}$, as for example,

$$f_n^{(k)}(x_o) = 0 \quad ; \quad f_n^{(k)}(x_f) = \delta_{nk}.$$

Three considerations dictate this choice of $\underline{x_1}$, $\underline{x_2}$. The first is simply that the above equations fulfill the true b.c. at $\underline{x} = \underline{x_o}$. The second is that the second of the equations is an ideal form for constructing solutions close to true scattering solutions at $\underline{x_f}$; exploding exponential solutions

$$B_n^k e^{+|k_n|x}$$

in virtual channels are forced to die out at $\underline{x} = \underline{x_f}$ in the first $\underline{n_{op}}$ independent solutions. Practical calculations on HOLJ and MOLJ verified that only $\underline{n_{op}}$ independent solutions need be generated and linearly combined, rather than $\underline{n_{tot}}$. The third consideration is that our b.c. allow us to write the discretized CC equations in a matrix form. Write the entire set of $\underline{f_n^{(k)}(x_i)}$ for all $\underline{n}$ and $\underline{i}$ as a single column vector $\underline{\underset{\sim}{X}^{(k)}}$ whose elements are

$$\left(\underset{\sim}{X}^{(k)}\right)_j = f_n^{(k)}(x_i) \tag{5}$$

where

$$j = (i-1)n_{tot} + n$$

$$x_i \in [x_1, x_{f-1}] .$$

Eqs. (4) can be written in the matrix form

$$\underset{\sim}{A}\ \underset{\sim}{X}^{(k)} = \underset{\sim}{b}^{(k)}$$

where

$$(\underset{\sim}{A})_{jj} = -\frac{2}{h^2} + k_n^2 - 2\mu V_{nn}(x_i) \qquad (6)$$

$$(\underset{\sim}{A})_{jk} = \frac{1}{h^2}\,, \quad k = j \pm n_{tot}$$

$$(\underset{\sim}{A})_{jk} = -2\mu V_{nm}(x_i)\,, \quad k = (i-1)\,n_{tot} + m$$
$$m \leq n_{tot}$$

$$(b)_j = 0\,, \quad j < (f-i)\,n_{tot}$$

$$(b)_j = \delta_{nk}\,, \quad j \geq (f-i)\,n_{tot}\ .$$

The matrix $\underset{\sim}{A}$ is seen to be banded with a half-bandwidth of $n_{tot}+1$ (note the relation of Eqs. (5), (6) to the original FD method). A very rapid and accurate routine has been coded (for the IBM 7094 originally, on which all our calculations were performed) by McCormack and Hebert (C. McCormack and K. Hebert, "Solutions of Linear Equations with Digital Computers", Technical Report, Engineering Division, California Institute of Technology, 1965, unpublished) for solving equations of the above form using a Gauss triangularization and elimination technique. Both core and disk storage are used, allowing large solution vectors (up to 16,000 elements). Our initial calculations proved to be of the same order of practicality as DRILL calculations.

For reduction of our primitive solutions to the proper pure scattering states by linear combination, see the first reference to Diestler and McKoy. In any event, given the final 'reflection coefficients" A_n^I for the true

scattering states, the probabilities of transitions P_{mn} from state m to n are calculated simply as

$$P_{In} = \frac{k_n}{k_I} |A_n{}^I|^2.$$

This formula follows directly from the definition of probabilities as ratios of incoming currents in I and outgoing currents in n.

a. Some Problems in Numerical Technique

Given an atom-diatom collision system, the parameters E, μ, and the parameters of the potentials V_{12}, V_I (henceforth called system parameters) are fixed. Several solution-method parameters remain to be chosen. The most obvious is n_{tot}, the number of channels retained in the expansion (1). Practical calculations carried out at energies E such that 2, 3, 4, 5, and 6 channels are open indicated that values n_{tot} = 4, 5-6, 7, 9, and 10, respectively, suffice to give transition probabilities converged to within one percent. These values are appropriate to the HOLJ and MOLJ models and should not be taken as general guides (the optimal number depends upon the degree of diabaticity in the collision and the relative spacing of the upper levels of vibration). A second parameter is the step size h in the difference equations. Experience indicated that a good choice is $h = 0.15/k_1$, where k_1 is the wavenumber of channel 1. The error introduced by keeping h this coarse, when compounded with the channel-truncation error, yielded a net error of less than one percent (relative) in the P_{In}. The

use of several coarser values of h with subsequent extrapolation (as in Diestler and McKoy) is more time-consuming for the same accuracy, and a like criticism applies to use of a coarser h with higher-order difference approximations to the CC d.e.'s.

A further set of parameters is the pair of limits x_o, x_f. The Lennard-Jones potential is singular at $x-y = 0$ but may be cut off at some b and set to a constant value for $x-y \leq b$. A good scheme is to cut off V_I when it reaches a magnitude of ten times the maximum kinetic energy (and is thus impenetrable to the particle even quantum-mechanically)

$$V_I \rightarrow 10\ (E-\epsilon_1)$$
$$=10\ (E-0.5).$$

A complementary choice of x_o is $x_o \simeq b - 3$. The value of x_f is strictly equal to infinity, since the Lennard-Jones potential is of infinite range. However, the CC equations effectively decouple to give free plane-wave $f_n(x)$ as of Eq. (2) when V_I drops to some small value. Decoupling occurs later (at larger x_f, smaller V_I) as the energy E approaches a threshhold of a channel from above, so the choice of x_f will depend upon the smallest wavenumber k_m in the problem at hand. To illustrate, two choices are

$$V_I(x_f) \approx 2.5 \times 10^{-6} \text{ when } k_m^2 \approx 0.05$$
$$V_I(x_f) \approx 2.0 \times 10^{-4} \text{ when } k_m^2 \gtrsim 0.35.$$

A final parameter is n_s, the number of linearly-independent solutions to be generated. This was set to n_{op} in all our

calculations for reasons noted earlier.

Regarding accuracy of the solutions $\underset{\sim}{X}^{(k)}$, there are two considerations in addition to the choices of parameters above. The first is the accuracy attainable in solution of the FDM equations (6) by Gauss' method. Tests were made using the feature of the routine which allows iterative improvement of the solutions. Basically, only small and uniform changes in the phases of the $f_n^{(k)}$ were noted in improved solutions, even for lengthy solution vectors near channel threshholds. This reveals an advantage of FDM, in that significant errors do not 'propagate'. The second consideration is the accuracy in evaluating matrix elements $V_{mn}(x)$ for the HOLJ and MOLJ models studied. Analytic forms do not exist and numerical quadrature must be used. Extensive trials showed that for the HOLJ case, where the oscillator eigenfunctions $\phi_n(y)$ are spatially compact, a twenty-point Hermite quadrature in y gave good results. For the MOLJ case, the eigenfunctions for higher n become quite diffuse, making something like our 181-point trapezoidal quadrature necessary. at least for $x < \sigma$ (the Lennard-Jones parameter). To save computer execution time, a series expansion of $V_I(x-y)$ in powers of $y-y_o$ (y_o is roughly the average location of the maxima in $\phi_n(y)$) was used for $x-y_o \geq \sigma$, yielding $V_{lm}(x)$ as a sum over moment integrals.

b. Similar Considerations for Diatom-Diatom Cases

For these cases, as noted in the text the CC

equations have exactly the same form as Eq. (14) of the text but the channel index $\underline{n}$ is really a double index $\underline{n_1 n_2}$ denoting the states of vibration in both collision partners. The total number of channels rises, and exactly which double channels are to be retained is a little tricky--the choice is discussed in the text and in Table I.there.

The discussion of section (a) on b.c. applied to the primitive solutions $\{\underline{f_n^{(k)}(x)}\}$ and the final physical solutions $\{\underline{F_n^{(I)}(x)}\}$ also holds for the diatom-diatom case. The primitive b.c. were slightly modified, however, to read

$$f_n^{(k)}(x_f) = \begin{cases} 0, & n \neq k,\ n > n_{op} \\ 0.1, & n \neq k,\ n \leq n_{op} \\ 1.0, & n = k\ . \end{cases}$$

We found a slight improvement in accuracy near threshholds over the original b.c. One problem peculiar to the case of identical diatoms and to the necessary b.c. is that the matrix $\underline{A}$ in the diatom-diatom analog of Eq. (6) is nearly singular due to the presence of equivalent channels $(\underline{n1, n2})$ $\leftrightarrow$ $(\underline{n2,n1})$. These channels are physically distinct; a transition from one to the other involves no conversion of translational into vibrational energy--it is a <u>resonant</u> transfer. However, their respective coupled equations differ mathematically only due to b.c. on the $\underline{f_m^{(k)}(x)}$. They would otherwise be related by a single permutation of terms on the right-hand side of Eq. (6). Without going into more

detail, we note that the $f_n^{(k)}(x)$ for equivalent channels n and n' become very similar for all but two values of the superscript k, and identical whenever k corresponds to a channel ($n3$, $n3$). The implications of this behavior for the FDM method of solution by Gauss' algorithm are that each initial solution vector $\underline{X}^{(k)}$ is accurate, but attempts to iteratively improve the solution lead to divergences. No practical problems were caused by this difficulty.

The solution method parameters h, x_o, x_f, and n_s are chosen by the criteria outlined in section (a). The goal of our calculations on the HOHOLJ model is to have probabilities P_{mn} of relative accuracy one percent. The choice of adjustable parameters given above can assure this goal for the energy range encountered, if the matrix elements $V_{nm}(x)$ are calculated with sufficient accuracy (perhaps 1 part in 10^4). These matrix elements require a two-dimensional numerical quadrature in the variables y_1, y_2. Each dimension was treated by twenty-point Hermite quadrature, as for the atom-diatom case. To cut down on computer execution time, the $V_{nm}(x)$ were tabulated on magnetic tape at a modest grid spacing $x = 0.20$, and each calculation of the solution vectors at a given energy used matrix elements interpolated cubically from this tabulation. The error added into the P_{mn} by interpolation error was about 0.01%.

c. Miscellany: Timings, Refinements, Relation to 3-D Scattering

Precise timings for calculations by our method are only of academic interest, while the order of magnitude and dependence on energy E (or equivalently, on n_{tot}) and on the complexity of the model are more generally significant. First, we note some typical compute times on an IBM 7094 (roughly the same speed as the new IBM 370/155). For the HOLJ model used here, the times are:

E	n_{tot}	t(sec.)
2.45	4	53
3.05	6	112
6.20	10	438

and for HOHOEXP (similar to HOHOLJ but using only trivial time for computing $V_{nm}(x)$ relative to actual Gauss solution; better indicator of the integrator per se):

2.46	9	127 .

Gordon's new integrator (ref. 24 of introduction) should cut these times by an average factor of about 20. Thus calculations with 40-50 channels are even feasible at the extreme, since all integrators' times increase roughly as n_{tot}^3. This is nothing to lament, really, since the detailed S-matrix for a large number of channels is not very meaningful for an understanding of collision processes--for the same reason that in statistical mechanics the trajectories of 10^{23} particles in a bulk system aren't meaningful: both are

filled with irrelevant detail, irrelevant for the aim of correlating molecular structure with properties. A further argument against large model problems is the rising proportion of computing effort going into computing just the V_{nm} matrix elements; for HOLJ these take about 50-70% of the total compute time, while for HOHOLJ they comsume fully 95%.

Before closing, we should like to mention two possible refinements to the scattering solutions; the second is of interest even for newer CC integrators. First, analogous to the use of higher-order predictor-corrector formulae in the straightforward CC integrators such as DRILL, the actual numerical integration scheme in FDM can be improved. An obvious action is switching to a five-point difference formula in discretization, possibly a Numerov formula. At the endpoints x_o, x_f, of course, we shall have to revert to the 3-point formula. We did not try this, as our total computing effort was modest as the method stood--and we may not even gain by increasing the mesh size h but doubling the matrix bandwidth to $2\ n_{tot} + 1$. Besides, Gordon's integrator has superceded all simple integrators.

The second refinement tested was a shortening of the distance in x, $x_f - x_o$, over which we propagate the solutions $f_n^{(k)}(x)$ before assuming they have attained their essential potential-free plane-wave form and proceeding to analyze them for the A_n^k, B_n^k and hence the transition probabilities. The common experience of investigators in

molecular scattering theory is that V_I must be down to the general magnitude of 10^{-4} energy (oscillator) units for the analysis and probabilities to be stable (to variations in the analysis point x_f, that is). We felt that the strong diabatic (transition-causing) couplings of channels might be completed (especially in systems with 'soft' interactions V_I) much earlier, say at x_d where $V_I \approx 0.1$. Analysis at x_d in an adiabatic basis for this x might be successful. This adiabatic basis of oscillator functions is parametric in x_d, i.e., it is $\phi_n(y|x_d)$, and each function is a solution of the equation

$$\left[-\tfrac{1}{2}\frac{d^2}{dy^2} + V_{12}(y) + V_I(x_d-y) - \bar{\epsilon}_n(x_d)\right] \Phi_n(y|x_d) = 0.$$

This basis of 'perturbed stationary states' must be solved for numerically in general, and definitely when V_I is a Lennard-Jones potential. To be brief, this analysis failed, for our HOLJ H_2-H_2 model at least. Perhaps diabatic coupling is strong even to low V_I for the harder potentials.

In closing, we should like to mention one point of interpretation of the one-dimensional (1-D) or collinear solutions: the wavefunction in our 1-D model is also the S-wave portion of the partial-wave expansion of the 3-D wavefunction, for a 'breathing sphere' (a collision system where there is no diatom-orientation- or angle-dependence in the interaction potential; implies a perfect but compressible sphere):

$$\psi^I_{3D}(x,y) = \sum_n \left\{ \delta_{nI} e^{ik_I z} + g_n(\theta) e^{ik_n r}/r \right\} \phi_n(y)$$

$$\left(H = -\frac{h^2}{2\mu}\nabla^2 + H^o(y) + V_I(r-y) \right)$$

$$= \sum_n \left[\frac{1}{r} \sum_l u^n_l(r) P_l(\cos\theta) \right] \phi_n(y),$$

where $u^n_l(r)$ satisfies

$$\left[\frac{d^2}{dr^2} - \frac{l(l+1)}{r^2} + k_n^2 \right] u^n_l(r) = 2\mu \sum_m V_{nm}(r) u^m_l(r).$$

Clearly for $l = 0$ (S-wave) this is our collinear collision equation of motion. What does this imply for the relation of the 1-D transition probabilities (pure numbers) to 3-D transition cross-sections (areas)? Now, the 3-D scattering amplitude $g_n(\theta)$ has the form

$$g_n(\theta) = \frac{1}{2ik} \sum_l (2l+1)(-1)^{l+1}(A^I_{n,l} - (-1)^l \delta_{nI}) P_l(\cos\theta)$$

where the $A^I_{n,l}$ are the simple generalization for the l-waves of the A^I_n of our S-wave. The 3-D differential cross-section is $\sigma_{In}(\theta) = \left| g^I_n(\theta) \right|^2$, and the total cross-section Q^{In}_{tot} integrated over angles θ is simply

$$Q^{In}_{tot} = \frac{\pi}{k_I^2} \sum_l (2l+1)(A^I_{n,l} - (-1)^l \delta_{nI})^2.$$

For $n \neq I$ and for S-wave scattering dominating, the total cross-section simplifies to

$$Q^{In}_{tot} \simeq \frac{\pi}{k_I^2} \left| A^I_{n,o} \right|^2 = \frac{\pi k_n}{k_I^3} P_{In}.$$

This is the result we seek; note that Q is an area, rightly.